# Carbon Nanotubes for Photoconversion and Electrical Energy Storage

A. C. Dillon*

*Center for Materials and Chemical Sciences, National Renewable Energy Laboratory, Golden, Colorado*

*Received October 4, 2009*

## Contents



## 1. Introduction

The majority of the world energy consumption is derived from fossil fuels. The conversion reactions required for retrieving energy from carbon resources result in the production of green house gases and subsequent global warming effects. Furthermore, the United States (U.S.) consumption of petroleum vastly exceeds its production, with the majority of the petroleum being consumed in the transportation sector. The severe environmental impacts of a petroleum-based society coupled with increasing dependency on foreign fuels dictates that alternative renewable energy resources be developed and implemented. The U.S. Department of Energy's (DOE's) Office of Energy Efficiency and Renewable Energy[1,2] and the Office of Basic Energy Sciences[3] are currently promoting the need both to rely on solar energy and also to implement efficient methods for electrical energy storage. However, significant scientific advancement is still required for the practical and safe deployment of both of these technologies. A detailed discussion of the benefits of transitioning to a solar-powered energy economy as well as the technical hurdles faced for the development of electrical energy storage systems, with a focus on vehicle technologies, is provided here. Many next-generation photovoltaic (PV) and electrical energy storage devices, such as Li-ion batteries and electrochemical capacitors, will be advanced as a result of new developments in nanotechnology. Carbon nanotubes (CNTs) have been widely studied since their discovery in 1991.[4] CNTs have highly unique electronic, mechanical, catalytic, adsorption, and transport properties, making them interesting for a variety of applications.[5−13] This review focuses on how both carbon multiwall nanotubes (MWNTs) and single-wall nanotubes (SWNTs) may be employed to improve upon state-of-the art photoconversion and electrical energy storage technologies.

Anne Dillon is a Principal Scientist at the National Renewable Energy Laboratory (NREL) in the Center for Materials and Chemical Sciences. Her research at NREL is focused on the synthesis and characterization of nanostructured materials, including single-wall and multiwall carbon nanotubes as well as metal oxide nanoparticles and, recently, silicon nanostructures and amorphous Si powders. The nanostructures are targeted for a variety of renewable energy applications, including vehicular electrical energy storage, electrochromic windows, and fuel cells. She received B.S. degrees in both chemistry and history from the Massachusetts Institute of Technology in 1988 and took a significant fraction of her history courses at Harvard University via cross registration. She received a Ph.D. in physical chemistry from Stanford University in 1993. She has over ninety peer-reviewed publications with over four thousand citations. She received an NREL Directors Award in 2004 for outstanding contributions to the development of new hydrogen storage materials. She was a guest editor for a special renewable energy edition of the *Journal of Materials Research* in 2005. She was invited by the National Academy of Engineering to participate in the American Frontiers of Engineering Symposium in 2006 and then later to organize an energy session at the U.S./Japan Frontiers in Engineering Symposium in 2009. She received an NREL Staff Award in 2009 for outstanding leadership in a variety of renewable energy fields. She was the Spring Materials Research Society Meeting Chair in 2010 and is presently editing an energy edition of the Materials Science Research Bulletin.

### 1.1. Energy Needs and Opportunities

In 2005 the entire world power consumption was approximately 13 terrawatts (TW), the equivalent of 87 billion barrels of oil. Also the U.S. represented only 4.6% of the world's population yet annually consumed ∼25% of the world's energy resources and was therefore the largest single energy consumer.[14] Over 80% of the world energy utilized is derived from fossil fuel resources.[15] Figure 1 displays a

* Corresponding author. E-mail: anne.dillon@nrel.gov.

10.1021/cr9003314 
Published on Web 09/14/2010

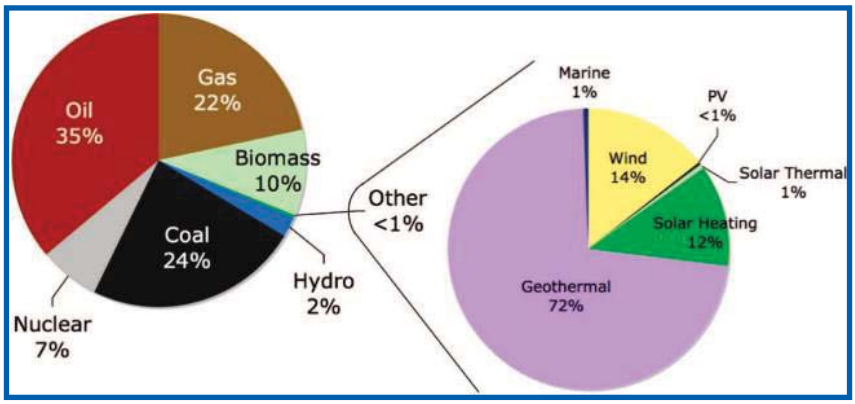


**Figure 1.** Breakdown of the 2005 world energy consumption, with the total energy consumed being ~13 TW and roughly the equivalent of 87 billion barrels of oil. (Reprinted with permission from ref 15. Copyright 2005 Materials Research Society.)

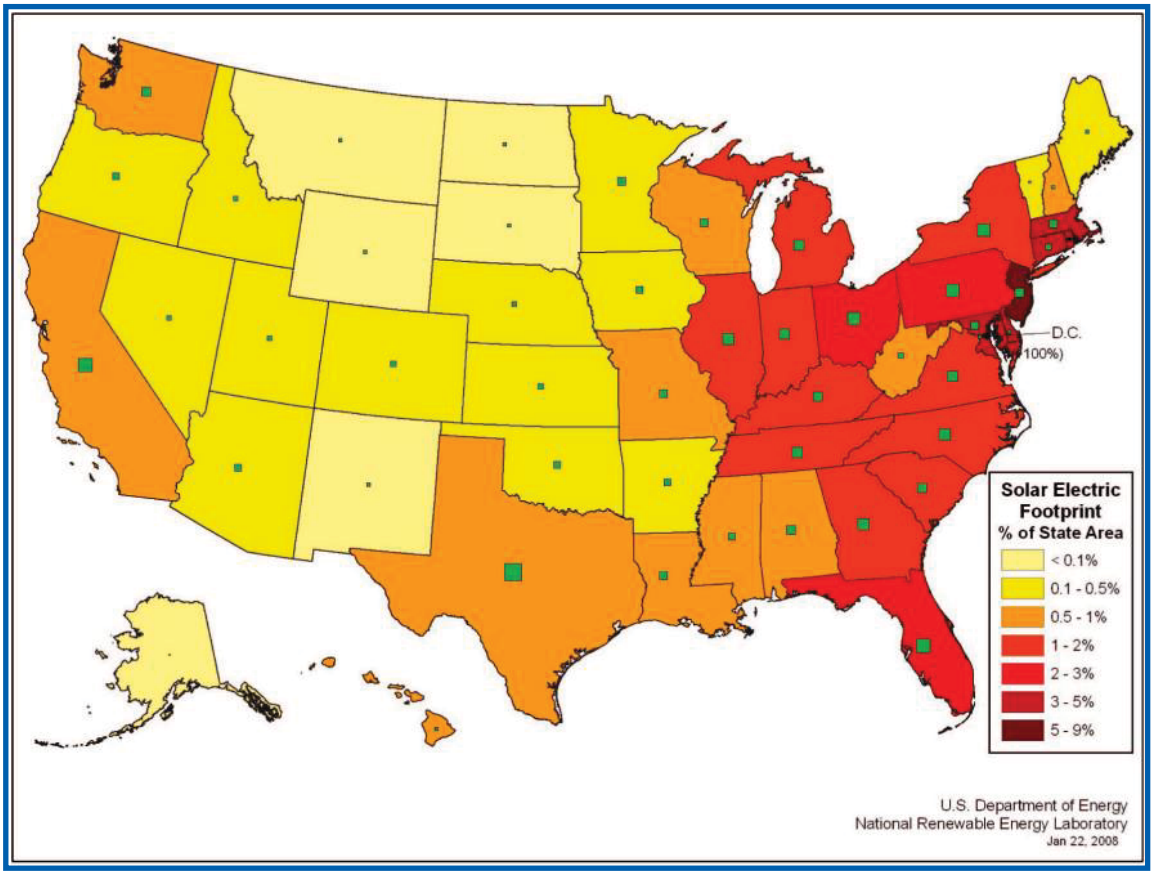


**Figure 2.** Land area required to provide 100% of U.S. energy needs from PV depicted by green squares. Solar electric footprint and color code are in the inset. (Courtesy Dr. James Ohi, NREL.)

pie chart breakdown of the 2005 world energy consumption. Note that 7% of the world energy use was derived from nuclear power. Nuclear power is desirable as long as the isotope uranium 235 ($U^{235}$) is employed.[16] However, a less than twenty year supply of $U^{235}$, which may be recovered at a reasonable cost, is available. It will then be necessary to employ breeder reactors. Unfortunately, the byproduct of this reaction is the very hazardous element, plutonium, $P^{239}$ ($U^{238} \rightarrow P^{239}$).[16] (The generation of plutonium, of course, requires a tremendous safety infrastructure and also dictates a need for moral leadership.) Note also in Figure 1 that 10% of the world energy consumption is derived from biomass. However, this is not nearly representative of what could be accomplished.[17] Finally, 2% of the energy consumption relies on hydroelectric sources and a mere 1% of the energy consumed is obtained from alternate renewable resources. A blowup of this tiny 1% fraction shows that both solar energy in the form of photovoltaics and wind power are drastically underemployed (Figure 1). These, of course, represent two renewable resources, of which there is an essentially infinite supply. For example, in Figure 2 the land area required to provide 100% of U.S. energy needs from PV is depicted by green squares in the American map. The inset in Figure 2 provides a color code showing the percent of each state's area that would be required to allow for the U.S. to operate using only PV power. In the worst cases, only 5−9% of the land area of any given state would be required for the state to be PV-powered. Also, in most cases, less than 1% of the state's land area is needed.

However, because PV is an intermittent energy source, it will also be necessary to implement electrical energy storage technologies so that PV can provide electricity at a significant scale. Analysis studies of the necessary electrical energy storage technologies that need to be developed to implement

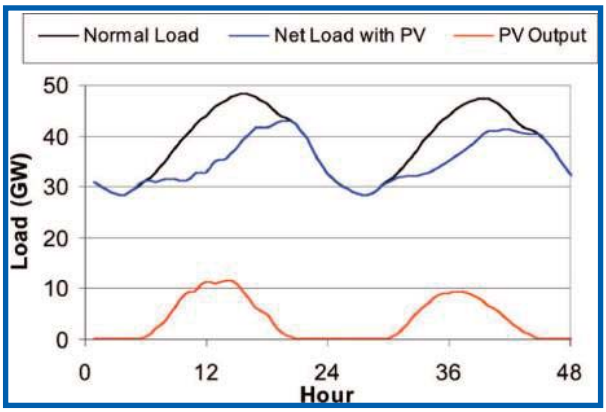


**Figure 3.** Example of PV supply with electricity demand in Texas during June. The simulated PV is supplying 10% of the energy demand. (Courtesy Dr. Paul Denholm, NREL.)

sustainable renewable energy resources are currently being performed.[18−20] For example, Denholm et al. explored the possibility of PV providing up to 50% of the energy required in Texas.[18] Figure 3 provides an example of a simulated PV supply with electricity demand in Texas during June.[18] In this case the simulated PV system is providing 10% of the region's energy demands. Note that even during the summer, in Texas, the peak demand for energy and the ability to provide PV energy when needed are somewhat out of phase, dictating a need for storage. The need for storage in the winter, of course, becomes even more important.[18] Several utility-scale energy-storage systems are currently being deployed, including pumped hydrostorage and compressed air energy storage. However, there are geographical constraints to utilize these simple technologies effectively.[19] Batteries are more scalable in size and do not depend on availability of water or air storage.[21,22] Furthermore, improved Li-ion batteries will enable the development of improved hybrid electric or plug-in hybrid electric vehicles (HEVs and PHEVs).[23] PHEVs can also be considered as electrical energy storage units if the PHEVs are "plugged-in" and charged during the day using PV power. In a subsequent section, the role carbon nanotubes may play in improving next-generation Li-ion batteries and electrochemical capacitors, for improved electric vehicles, is discussed.

## 1.2. Carbon Single-Wall Nanotube Background

Single-wall carbon nanotubes were first synthesized by the coevaporation of a cobalt catalyst and graphite in an electric arc.[24,25] Every SWNT can be considered to be a unique molecule, with different physical properties, depending on its $(n,m)$ indices, where the chiral vector $\vec{C}_{nm}$, whose magnitude denotes the nanotube circumference, is given by $\vec{C}_{nm} = n\vec{a}_1 + m\vec{a}_2$, in which $(\vec{a}_1,\vec{a}_2)$, are the unit vectors of the 2D graphene lattice. From the chiral vector $\vec{C}_{nm}$, the nanotube diameter $(d_t)$ and the chiral angle $(q)$ can be written as

$$d_t = a(n^2 + nm + m^2)^{1/2}/\Pi \text{ in which } a = 0.246\ nm \text{ and}$$
$$q = \tan^{-1}\sqrt{3}m/(2n + m)^7$$

Figure 4 illustrates how an SWNT may be indexed by two unique integers $(n,m)$.[26] A graphene sheet segment with indexed lattice points is depicted. Nanotubes designated $(n,m)$ are obtained by rolling the sheet from (0,0) to $(n,m)$ along a roll-up vector, $\vec{C}_{nm}$. The chiral angle, $q$, is measured between the roll-up vector and the $(0,m)$ zigzag axis. At present, there is no simple way to grow a unique $(n,m)$ SWNT sample or to separate an aliquot of one type of an $(n,m)$ nanotube from an ensemble of SWNTs containing a distribution of diameters and chiralities. Although obtaining a single aliquot of one $(n,m)$ nanotube is not necessary to improve photoconversion and energy storage processes, it is still necessary to obtain nanotubes that are free of non-nanotube carbon impurities and metal catalyst particles (employed to make SWNTs). In some cases, it is also necessary to obtain SWNTs that are primarily metallic or semiconducting. Purification and separation techniques are continuously evolving and are discussed in more detail below.

In the early arc-generated nanotube material, the SWNT fibers typically consisted of 7−14 bundled SWNTs, with the individual tubes being 1.0−1.5 nm in diameter. The early arc-generated materials also contained relatively low weight percent densities of SWNTs. An improvement in the nanotube yield was observed by changing the metal catalysts employed in the arc-technique.[27] Figure 5a displays a transmission electron microscope (TEM) image of a typical arc SWNT material generated with an iron catalyst.[28] Note that the nanotube bundles are relatively small (containing ∼3−5 nanotubes). Single wall carbon nanotubes were later produced at much higher yield by the method of laser vaporization.[29] Crystalline ropes micrometers in length containing 10−100 s of individual SWNTs were easily obtained.[30] Figure 5b shows a typical TEM image of crude laser-generated material produced with an Alexandrite laser operating at ∼45 W/cm$^2$, with Co and Ni at 0.6 at % each and an external furnace temperature of 1200 °C.[31] Note the large, very long bundles of SWNTs present in Figure 5b. Although there is a high density of SWNTs (30−40 wt %), non-nanotube carbon impurities, as well as metal catalyst particles, are still clearly visible in the TEM image. Laser-generated single-wall carbon nanotubes typically have low defect concentrations,[32] making them easier to purify, since they are not as likely to be destroyed by the acids generally employed to remove metal catalyst particles. For example, SWNT material initially generated with a Nd:YAG laser[33] operating at 23 W/cm$^2$, with Co/Ni catalysts at 0.6 at %, was reported to be purified via refluxing in 15% $H_2O_2$ for 3 h at 100 °C to remove the non-nanotube carbon. The metal catalyst particles were then removed by sonication in an HCl/water mixture.[33] In a similar report, laser-genrated SWNTs were purified with dilute $HNO_3$ to remove the metal catalyst particles and then burned in air at 550 °C to remove the non-nanotube carbon.[34] However, the laser technique is often considered to be too expensive to be industrially scalable.

Consequently, numerous research groups have turned to the development of chemical vapor deposition (CVD) as a potentially low-cost scalable technique for the production of SWNTs. In 1996, SWNT growth employing chemical vapor deposition on a supported catalyst was demonstrated as a promising route to nanotube production.[35] Multiple reports quickly followed, further establishing CVD as a viable large-scale production process.[36−45] Typically, CVD materials contain more metal and often smaller and shorter SWNT bundles than those produced in the laser processes. Figure 5c shows a TEM image of commercially available CVD material produced by a high pressure carbon monoxide (HiPCO) process.[42] CVD production of isolated nanotubes has been achieved on oxidized silicon substrates using an iron catalyst.[46] Additionally, isolated SWNTs have been generated in the gas phase by the technique of hot wire

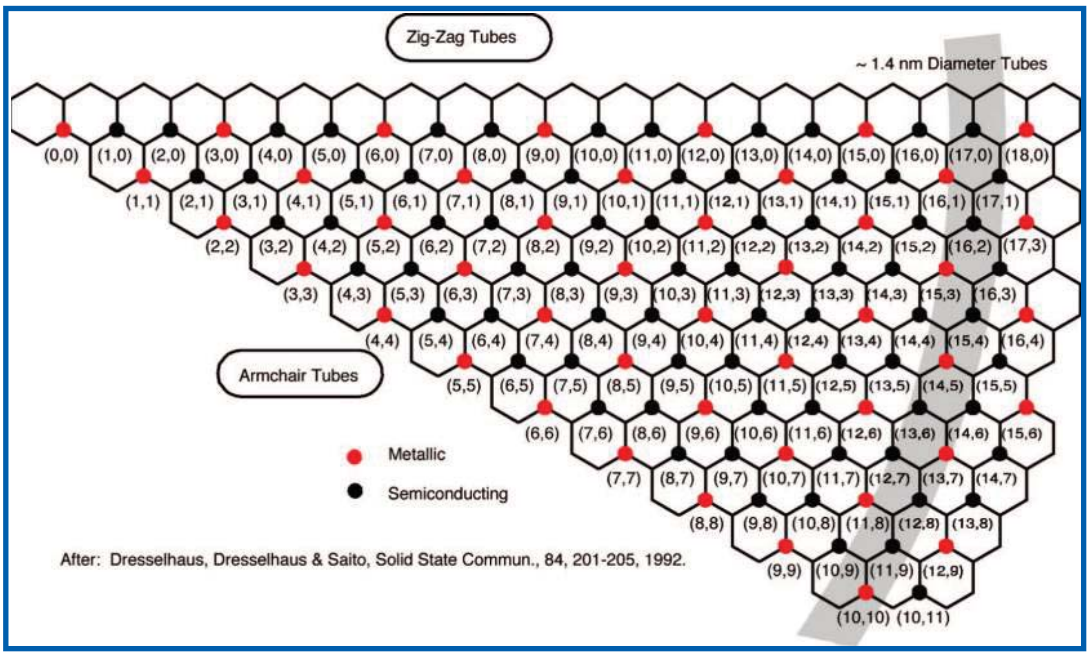


**Figure 4.** Illustration of how a SWNT may be indexed by two unique integers (*n*,*m*). (Reprinted with permission from ref 26. Copyright 1992 Elsevier Ltd.)

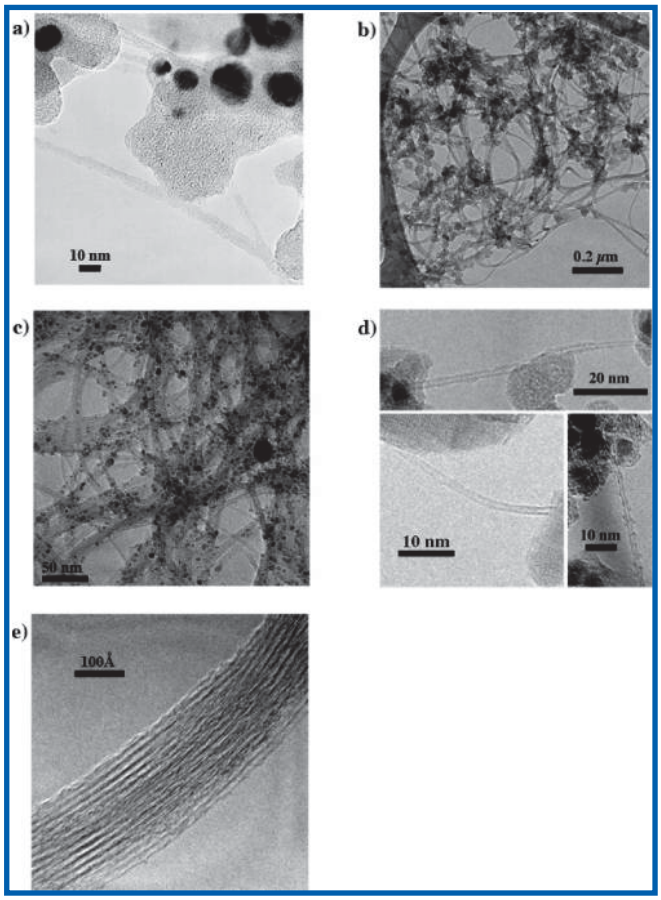


**Figure 5.** TEM images of bulk SWNT materials showing (a) typical arc-material generated with a Co/Ni catalyst mixture. (b) Alexandrite laser-generated crude material produced with ~45 W/cm$^2$ and a Co/Ni catalyst mixture at 1200 °C. (c) commercially available CVD material produced by the HiPCO process. (d) Isolated SWNTs produced by a continuous HWCVD process where ferrocene is employed to supply the metal catalyst. (e) Bundle of purified laser-generated SWNTs. (Reprinted with permission from ref 5. Copyright 2004 American Scientific Publishers.)

chemical vapor deposition (HWCVD).[13,47] Figure 5d shows high-resolution TEM images of isolated SWNTs produced by this HWCVD process. For comparison, a high resolution TEM image of a bundle of purified laser-generated SWNTs is also provided in Figure 5e.[9] A multistep process for the purification of HiPCO CVD-generated nanotubes was reported in 2001.[48] Recently, K. E. Hurst reported a simple "laser cleaning" method than can be employed to purify a host of CNT materials.[49]

As mentioned previously, for some photoconversion and energy storage applications, it is necessary to obtain SWNT materials that are comprised of predominantly metallic or semiconducting nanotubes. Metallic (M) tubes require the condition $(n - m) = 3z$ to be satisfied, where $z$ is an integer, while semiconducting (S) tubes require the condition $(n - m) = 3z \pm 1$. Several experimental methods have been used to produce M/S separations, including chemical affinity methods,[50] DNA-based chromatography methods,[51,52] and dielectrophoresis.[53] Recently, a simple centrifugation process was demonstrated to obtain efficient separation of metallic and semiconducting tubes.[54] Also in 2009, Tanake et al. reported a novel method to separate metallic and semiconducting single-wall carbon nanotubes with high purities using an agarose gel. When a SWNT/sodium dodecyl sulfate dispersion was applied to a column containing agarose gel beads, semiconducting SWNTs were trapped by the beads, while metallic SWNTs passed through the column. Futhermore, the semiconducting SWNTs, adsorbed to the beads, were eluted with sodium deoxycholate solution, and the column could then be used for repeated separation.[55] The separation efficiency can be easily characterized using Raman[5] and absorbance[56] measurements. These advancements have allowed for the incorporation of M or S phase pure SWNTs into many technologies such as photovoltaic devices, Li-ion batteries, and ultracapacitors.

## 1.3. Carbon Multiwall Nanotube Background

Multiwall carbon nanotubes were discovered by Iijima in 1991 while vaporizing carbon in an electric arc[4] and were

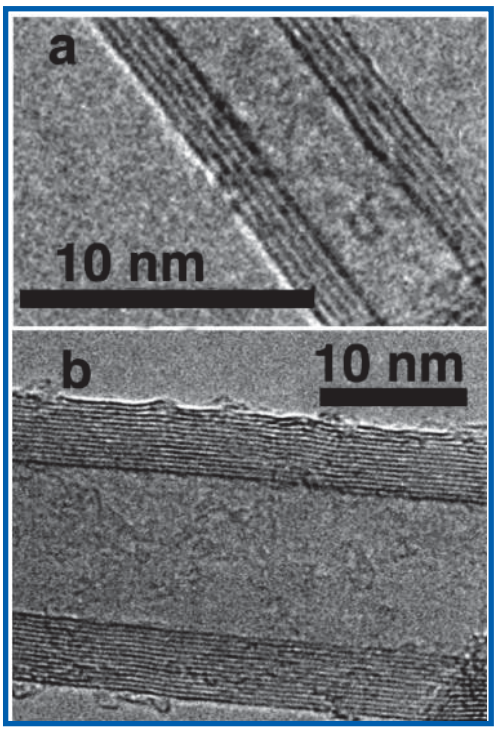


**Figure 6.** TEM images of MWNTs (a) showing that the distance between layers of the MWNTs measures ~0.34 nm and (b) depicting an MWNT with ~15 concentric shells. (Reprinted with permission from ref 58. Copyright 2003 American Chemical Society.)

then produced at higher yield by increasing the pressure of the helium gas atmosphere.[57] Carbon MWNTs typically have inner diameters of ~3−20 nm and are then surrounded by concentric graphene sheets with an interstitial spacing between the sheets of ~3.4 Å. The number of concentric graphene sheets can range from 2 to ~100. When there are only two concentric layers, the MWNTs are then referred to as double-walled nanotubes (DWNTs). High resolution TEM images of MWNTs are provided in Figure 6.[58] In Figure 6a the high-resolution TEM image clearly shows that the distance between layers of the MWNTs measures ~3.4 Å. Figure 6b depicts a MWNT with ~20 concentric shells. Carbon multiwall nanotubes have electronic properties similar to those of graphite and are thus semimetals. They are promising for multiple applications including strong composite materials, field emission displays, adsorbents for gas separation or storage,[59−66] as well as PV and electrical energy storage devices that are reviewed in the subsequent sections.

Similar to SWNTs, a continuous low-cost production method producing MWNTs that are easily purified is required for MWNTs to be incorporated in emerging technologies. In 1997[67] and 1998,[68] ferrocene was utilized as a gas-phase catalyst in a CVD process for continuous MWNT formation from methane at 1150 °C. However, the 1997 study reported materials containing more amorphous carbon than arc-generated MWNTs, presumably due to a lower synthesis temperature than that achieved in the arc process.[67] In the 1998 study, the outer layers of the tubes were not graphitic,[68] making them more difficult to purify. Later, ferrocene and ethylene were employed in CVD of MWNTs between 650 and 950 °C.[69] Again, carbon impurities were observed at high-density. The authors concluded that further work was necessary to improve the nanotube microstructure and yield.[69] High-purity aligned, graphitic MWNTs were synthesized via decomposition of a ferrocene-xylene mixture at ~675 °C. However, although the catalyst was supplied in the gas-phase, nucleation of tube growth occurred only for iron species deposited on a quartz substrate, resulting in a surface growth mechanism and limiting yields to available surface area.[70]

Chemical vapor deposition techniques employing benzene pyrolosis[71] and the decomposition of ethylene[72] and acetylene[73] on supported metal catalysts have been demonstrated as viable large-scale production methods. MWNTs have also been grown on supported metal particles or films via CVD,[74−78] plasma-enhanced CVD,[79−89] hot-wire chemical vapor deposition,[90,91] and plasma-enhanced HWCVD methods.[92,93] One HWCVD report employed evaporation of the Fe−Cr filament to supply a gas-phase catalyst, resulting in MWNTs with a high density of structural defects and significant carbon impurities.[94] Although more research was deemed necessary, this method had potential for large-scale production, since it was not substrate dependent. In 2003, the first continuous high-density MWNT formation of graphitic MWNTs with minimal non-nanotube carbon impurites was demonstrated with HWCVD employing methane as the carbon source and ferrocene as a gas-phase catalyst.[58] The metal catalyst impurities were simply removed via refluxing in dilute $HNO_3$.[58]

## 2. Nanotubes for Improved Photovoltaic Devices

The highly unique physical properties of carbon nanotubes have been demonstrated for optoelectronic[95] and photonic applications including photovoltaic devices.[96−98] For example, nanotubes have been matched with an inorganic layer to create heterojunction solar cells. Carbon nanotubes have also been employed in PV devices to improve both exciton generation and transport of photoexcited carriers. In many instances, nanotubes have been demonstrated as either electron donors or acceptors in novel organic photovoltaic (OPV) technologies. Finally, very thin transparent films of nanotubes have been explored as transparent conducting contact layers for a variety of PV or other optoelectronic devices. A detailed overview of these research efforts is provided below.

### 2.1. Heterojunctions and Mechanistic Characterization

There has been a significant body of work devoted to the creation of heterojunction solar cells that contain a nanotube layer as well as an inorganic layer. For example, in 2006 poly(3-hexylthiophene)/*n*-Si heterojunction solar cells were studied with and without incorporation of double walled carbon nanotubes in the polymer. The authors reported the power conversion efficiency, open circuit voltage ($V_{oc}$), short-circuit current density ($J_{sc}$), and fill factor to be 0.026%, 0.446 V, 0.3398 mA/cm$^2$, and 0.17, respectively, for a nonoptimized cell containing DWNTs, where reference cells without nanotubes showed inferior performance.[99] In a more promising example, various CNTs were coupled with $ZnP^{8-}$, and the photocurrent response to visible light was examined.[100] Figure 7 illustrates the individual steps that take place in the reported CNT/pyrene$^+$/$ZnP^{8-}$ photoconversion process. The optimized hybrid approach resulted in monochromatic power-conversion efficiencies of up to 10.7% for a MWNT/pyrene$^+$/$ZnP^{8-}$ stack.[100]

In 2007 photoelectrochemical solar cells were constructed with “stacked-cup” carbon nanotubes on optically transparent

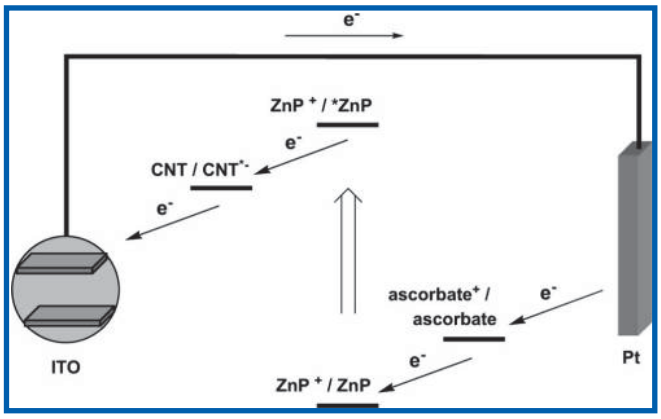


**Figure 7.** Schematic illustration of photocurrent generation in ITO-electrodes covered with a single CNT/pyrene$^{+}$/ZnP$^{8-}$ stack. (Reprinted with permission from ref 100. Copyright 2006 Wiley-VCH Verlag GmbH & Co. KGaA.)

electrodes ($SnO_2$). For an optimized film, a maximum incident photon to photocurrent efficiency of 19% was attained with the power conversion efficiency determined to be 0.11%.[101] Also in 2007, the occurrence of photoinduced electron transfer in donor−acceptor self-assembled zinc naphthalocyanine (ZnNc) or zinc porphyrin (ZnP) single-wall carbon nanotube hybrids was demonstrated.[102] Nanosecond transient absorption spectra revealed that the photoexcitation of the ZnNc or ZnP moiety resulted in one-electron oxidation of the donor unit with a simultaneous one-electron reduction of the SWNT.[102]

In 2008 a mini-arc plasma method was demonstrated to produce silicon nanocrystals at atmospheric pressure directly from solid silicon precursors.[103] The product silicon nanocrystals were then assembled on the external surface of MWNTs to form hybrid nanostructures. The absorption properties of both the silicon nanocrystals and the Si-MWNT hybrid structures were then characterized. Quantum confinement effects were observed, suggesting that both the silicon nanocrystals and the hybrid Si-MWNT nanostructures are promising for optoelectronic applications.[103] Finally, solar cells, based on high-density *p*−*n* heterojunctions between single wall carbon nanotubes and an *n*-type silicon wafer, were demonstrated.[104] Chemical modification of the SWNT coating with thionyl chloride was found to significantly increase the photoconversion efficiency by more than 45%, via adjustment of the Fermi level and a corresponding increase in the carrier concentration and mobility. (Electron−hole pairs were optically excited in the numerous heterojunctions formed between thionyl chloride-treated SWNTs and the *n*-type silicon substrate, and then they were transported through SWNTs, holes, and *n*-type Si, electrons, respectively.)[104]

## 2.2. Exciton Generation and Transport

Carbon nanotubes have also been demonstrated to improve light harvesting capabilities,(exciton generation) and/or to facilitate charge transport in a variety of photoconversion processes. For example in a seminal 2006 paper T. Hasobe et al. reported the construction of photochemical solar cells from assemblies of SWNTs and protonated porphyrin on nanostructured $SnO_2$ electrodes.[105] The organized assemblies were shown to be photoactive, absorbing strongly at visible wavelengths with an incident photon to photocurrent efficiency of 13%. Femtosecond pump−probe spectroscopy confirmed the decay of the excited porphyrin upon electron injection into SWNTs. The SWNTs were shown both to promote photoinduced charge separation and to facilitate charge transport.[105] Shortly thereafter, functionalized carbon nanotubes were demonstrated as support architectures to anchor semiconductor ZnO nanoparticles.[106] Upon excitation with UV light, charge separation was induced in the ZnO particles and electrons were injected with a rate constant of $1 \times 10^8$ s$^{-1}$. Both emission spectroscopy and photoelectrochemical measurements confirmed that the conducting carbon nanotube scaffolds facilitated charge collection and charge transport in the nanotube−ZnO composite film. Figure 8 displays a schematic representation of (a) photoinduced charge injection from an excited semiconductor particle into an SWNT and (b) the SWNT as a conducting scaffold to transport photogenerated charge carriers in the photoelectrochemical cell.[106]

Also in an OPV device, MWNTs were demonstrated as both exciton dissociation sites as well as hopping centers for hole transport.[107] Similarly, charge transfer between SWNTs and attached CdSe quantum dots was reported.[108] Later in 2008 an *in situ* growth deposition process for ZnO quantum dots on the surface of MWNTs was realized via a mild solution-processing method. The MWNT/ZnO quantum dots exhibited improved photoinduced charge separation and transport of carriers to the collection electrode.[109] The charge transfer efficiency was significantly increased by more than 90% due to the conjugation of ZnO quantum dots with the MWNTs (confirmed by photoluminescence measurements). The power conversion efficiency for this MWNT/ZnO quantum dot system was measured to be above 1%.[109]

In 2007 J. Wei et al. reported a very interesting DWNT solar cell[110] where the double-walled carbon nanotubes served both as photogeneration sites and as the charge carrier collection/transport layer. The solar cell consisted of a semitransparent thin film of nanotubes that were coated on an *n*-type crystalline silicon substrate to create a high-density *p*−*n* heterojunction between the nanotubes and the *n*-type Si, allowing for electron (Si) and hole (DWNT) pair formation. The initially reported measurements revealed a power conversion efficiency of >1%. The devices were distinct from previously reported organic solar cells where conjugated polymers were employed to generate the excitonic states.[110] Figure 9 displays a schematic illustration of the fabrication process employed to make the aforementioned DWNT/*n*-type Si solar cell. The as-grown DWNT films were suspended in a water solution, and a conformal coating of the DWNTs on a patterned Si substrate was achieved.[110]

In 2008 a three-dimensional solar cell structure was constructed by depositing a cadmium telluride thin film on carbon nanotube towers.[111] The nanotube towers acted as both a scaffold and an electrical interconnect. Furthermore, reflection of photons between the towers was reported to increase the absorption efficiency.[111] In 2009 enhanced photoconductivity was reported for aligned SWNT films.[112] Finally, SWNTs were reported to serve both as photogeneration sites and as charge carriers in an SWNT/*n*-type Si heterojunction solar cell.[113] The previously reported chemical modification method of the SWNTs by thionyl chloride[104] was shown to increase the conversion efficiency by more than 50% compared to the unmodified SWNTs. A power conversion efficiency of above 4% for the $SOCl_2$-treated SWNT cell was observed.[113]

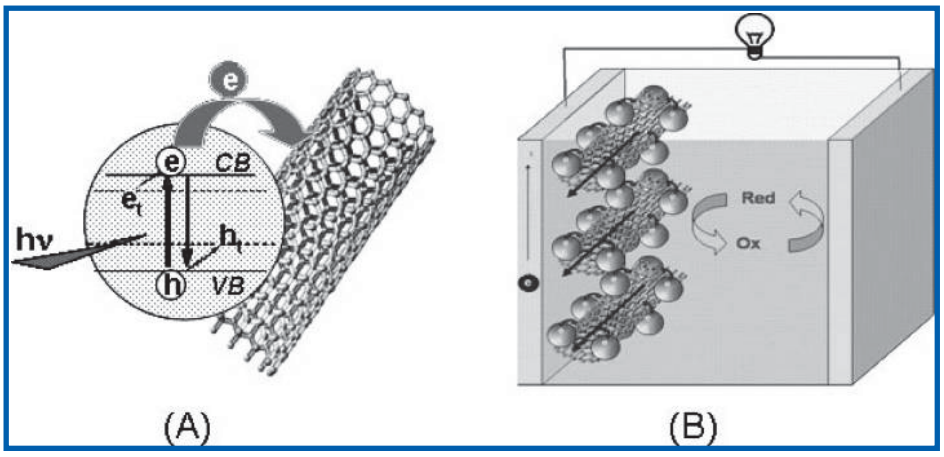


**Figure 8.** Schematic representation of (a) photoinduced charge injection from an excited semiconductor particle into a SWNT and (b) SWNTs as a conducting scaffold to transport photogenerated charge carriers in a photoelectrochemical cell. (Reprinted with permission from ref 106. Copyright 2007 Wiley-VCH Verlag GmbH & Co. KGaA.)

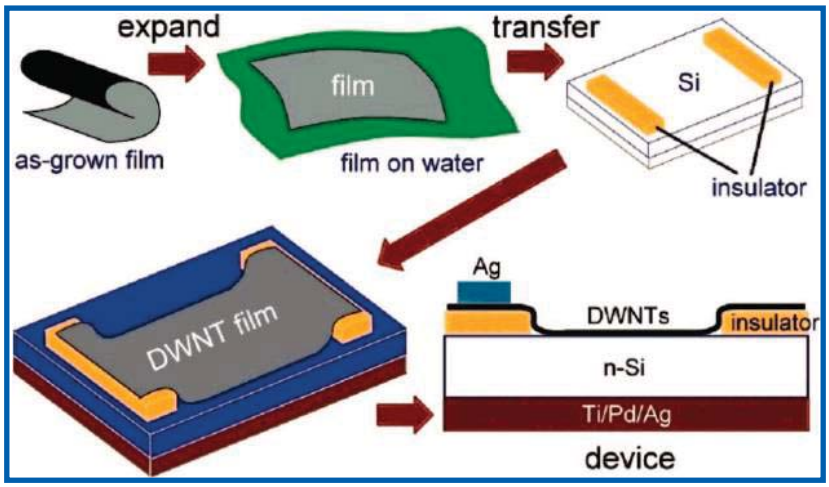


**Figure 9.** Schematic illustration of the fabrication process employed to make a DWNT/*n*-type Si solar cell. (Reprinted with permission from ref 110. Copyright 2007 American Chemical Society.)

## 2.3. Organic Photovoltaic Devices

The demand for organic photovoltaic technologies is rapidly increasing because the devices are made from abundant elements and are also flexible and light, providing for facile installation. Thus, OPV technologies may be especially useful for large-area applications. Organic solar cells are generally comprised of organic molecules[114,115] and conjugated polymers[116,117] and internal donor−acceptor polymer networks.[118] There is also a need for improving the efficiency of OPV cells. In 2007 the National Renewable Energy Laboratory (NREL) certified that Plextronics Inc. has an OPV technology that has achieved a world-record efficiency of 5.4%.[119] However, many OPV devices that are still under investigation have an efficiency of ∼2.5%.[120] (The standard single-junction silicon devices are approaching the theoretical limiting efficiency of 31%.[121]) Recently, the unique properties of carbon nanotubes have been probed in order to demonstrate CNTs as potential candidates for improving OPV devices. In a variety of cells, carbon nanotubes have been employed as either electron acceptors or donors.

For example, in 2003, Kymakis et al. studied SWNTs as electron acceptors in OPV devices with the donor (polymer) consisting of poly(3-octylthiophene) (P3OT).[122] In this report, the open circuit voltage of the device was found to be 0.75 V, which is larger than the theoretical limit calculated with a metal−insulator−metal model. The high $V_{oc}$ was found to be weakly dependent on the negative electrode work function. The results therefore suggested that the metal negative electrode formed an ohmic contact to an SWNT percolation path.[122] Also, low concentrations of MWNTs (∼1 wt %) were uniformly distributed within the donor layer of a heterojunction organic solar cell and were shown to reduce the cell series resistance without compromising cell shunt resistance, resulting in an increase in the cell fill factor of 50−60%.[123]

An extensive and thorough article in 2006 reported[124] a fabrication method to utilize either SWNTs or MWNTs to improve OPV devices. Solutions with regioregular poly(3-hexylthiophene) (P3HT) and a fullerene derivative, 1-(3-methoxycarbonyl)propyl-1-phenyl[6,6]$C_{60}$ (PCBM), were prepared with a spin-coating technique that enabled precise control of the ratio of carbon nanotubes to the P3HT/PCBM mixture and to allow for homogeneous dispersion of the CNTs throughout the matrix. It was then possible to examine the short circuit current with specific concentrations of CNTs. For example, Figure 10 shows the evolution of $J_{sc}$ as a function of the SWNT concentration in the P3HT/PCBM (1:1) active layer for as-made cells and after thermal post-treatment at 80 °C for 5 min. The authors reported that the best OPV device was fabricated with a P3HT/PCBM (1:1) mixture with 0.1 wt % MWNTs. This optimized cell had a

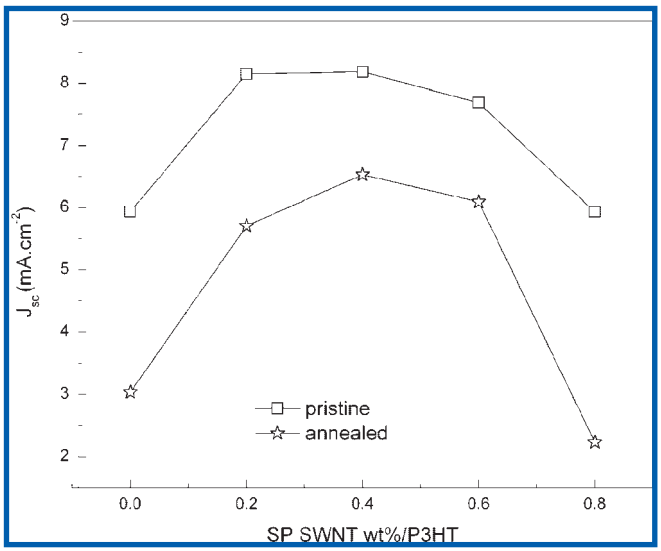


**Figure 10.** Evolution of $J_{sc}$ as a function of SWNT concentration in a P3HT/PCBM (1:1) active layer for as-made cells and after thermal post-treatment at 80 °C for 5 min. (Reprinted with permission from ref 124. Copyright 2007 Wiley-VCH Verlag GmbH & Co. KGaA.)

$V_{oc}$ of 0.57 V, a $J_{sc}$ of 9.3 mA cm$^{-2}$, and a fill factor of 0.384, which lead to a conversion efficiency of 2.0%.[124]

In a later report, a covalent modification of SWNTs with thiophene groups located at the edges and at defects was demonstrated to modify the interaction with the polymer matrix and allow for uniform SWNT dispersion.[125] Also, a novel immobilized fullerene−single-wall carbon nanotube ($C_{60}$-SWNT) complex was synthesized via a microwave induced functionalization approach. As compared to a control device with only $C_{60}$, the addition of SWNTs resulted in an improvement of both $J_{sc}$ and the fill factor.[126] Additionally, a uniform distribution of MWNTs in polymer matrixes was achieved by the addition of functional groups and electrostatic attachment of polyelectrolyte poly(dimethyldiallylamine) chloride to the nanotube surface.[127] In 2008 it was clearly demonstrated that energy transfer occurs between semiconducting organic polymers and SWNTs when the polymer is photoexcited, by monitoring the near-IR luminescence intensity from the nanotubes as a function of excitation wavelength.[128] Finally, very recently, Fanchini et al. reported the fabrication of organic solar cells utilizing SWNT thin films as the hole conducting electrodes. The authors concluded that, in addition to the transparency and sheet resistance (of the nanotube conducting layer that is discussed in detail below), factors such as the optical anisotropy of the SWNT networks must be considered prior to incorporation in optical devices.[129]

## 2.4. Transparent Conducting Contact Layers

Most PV devices require a transparent conducting contact layer, and the material that is typically employed is indium tin oxide (ITO). Superior performance satisfying the metrics of both high transparency and high conductivity for the ITO layer was demonstrated decades ago.[130] However, with the increasing demand for PV-power, it is necessary to develop transparent conducting contacts that perform as well as ITO but do not rely on the utilization of a high-cost element such as indium. Figure 11 displays the relative atomic abundance of elements in the earth's crust.[131] In general, the material cost is directly proportional to the elemental abundance. Thus, for large-scale applications, only elements appearing in the green or light green shaded area should be employed (Figure 11).

There has also been a considerable body of work to demonstrate that thin films of carbon SWNTs could replace ITO in many PV devices. In a seminal paper by Z. Wu et al.,[132] a simple vacuum filtration process was demonstrated for the fabrication of ultrathin, transparent, optically homogeneous, electrically conducting films of pure single-walled carbon nanotubes. In addition, the transfer of those films to various substrates was also performed. With equivalent sheet resistance to ITO, the films exhibited optical transmittance comparable to that of commercial ITO in the visible spectrum but far superior transmittance in the 2- to 5-$\mu$m infrared spectral band.[132] Shortly thereafter, strong transparent MWNT sheets were synthesized with a simple method, allowing for facile incorporation into a variety of devices.[133] These same MWNT sheets were then demonstrated in an OPV device that had an overall efficiency of ∼2%.[134,135]

In 2004 the group of George Gruner performed a detailed study of ultrathin, uniform single-walled carbon nanotube networks of varying densities fabricated for application as thin film transparent conducting networks. Measurements of the sheet conductance as a function of nanotube network (NTN) density showed 2D percolation behavior.[136] The nanotube films were fabricated by the vacuum filtration method, and it was demonstrated that, by changing the amount of the filtered nanotube solution, the films could be created such that the networks allowed for 2D percolation. Figure 12 displays scanning electron microscope (SEM) images of the nanotube networks on alumina substrates. Figure 12 a shows the NTN resulting from filtering 7 mL of a nanotube solution. The network is near the percolation threshold and has few or no percolative paths through the sample. For the film in Figure 12 b, 10 mL of SWNT solution was filtered and the NTN network was then above the percolation threshold, having several parallel pathways, allowing conduction across the film. For a film resulting from 400 mL of solution, the NTN became several layers thick (Figure 12 c).[136] In 2006 Gruner then wrote an applications review article for SWNT films as transparent conducting contacts for a variety of applications including "smart windows"[137−140] and organic solar cells.[141]

Also in 2006 a group at the National Renewable Energy Laboratory reported two viable organic excitonic solar cell structures where the conventional ITO hole-collecting electrode was replaced by a thin single-wall carbon nanotube layer.[142] Furthermore, in 2006 a Stanford group collaborating with Gruner reported an organic solar cell with an efficiency of ∼2.5% while using SWNTs as the transparent electrode.[143] Figure 13 shows the wavelength dependence of the optical transparency of the 30-nm-thick SWNT network in this cell with 200 Ω/square sheet resistance in the visible and infrared region. The spectrum for ITO, for which a peak in the transparency is observed at 550 nm is also provided. The nanotube network retains high transparency toward the near IR part of the electromagnetic spectrum.[143] In 2007 another NREL group reported single-wall carbon nanotube networks as a transparent back contact in CdTe solar cells.[144] The structure of the CdTe device with the NTN contact is provided in Figure 14.[144] Finally, the replacement of transparent conductive oxides by SWNTs in Cu(In,Ga)$Se_2$-based solar cells was also demonstrated at NREL in 2007.[145]

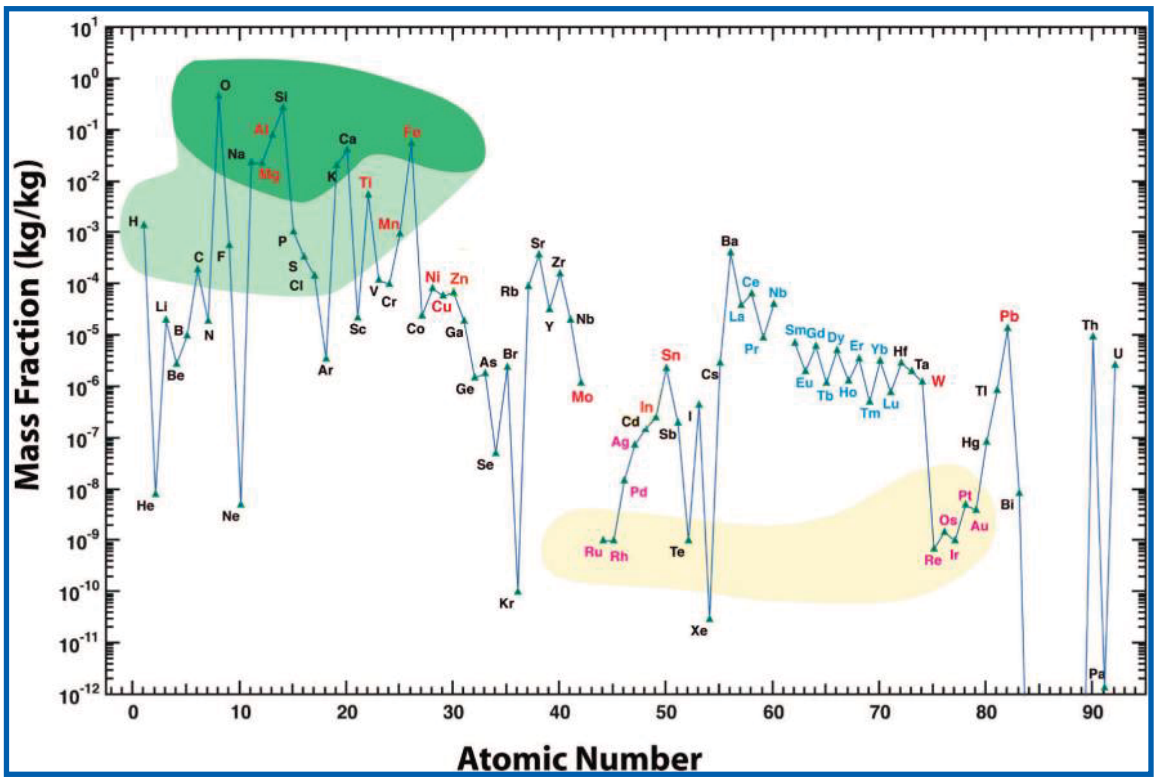


**Figure 11.** Schematic illustration of elemental abundance in the earth's crust. The elements in the dark green area are highly abundant and may be used for most large-scale applications with the elements in the light green area also generally being cost-effective for large-scale applications. The highly expensive and precious metals are highlighted in cream. (Reprinted from ref 131. USGS 2002.)

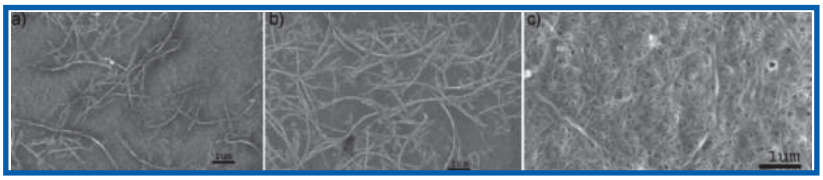


**Figure 12.** SEM images of NTNs resulting from (a) filtering 7 mL of a nanotube solution; (b) 10 mL of the NTN network then above the percolation threshold, having several parallel pathways, allowing conduction across the film, and (c) 400 mL of solution where the NTN became several layers thick. (Reprinted with permission from ref 136. Copyright 2004 American Chemical Society.)

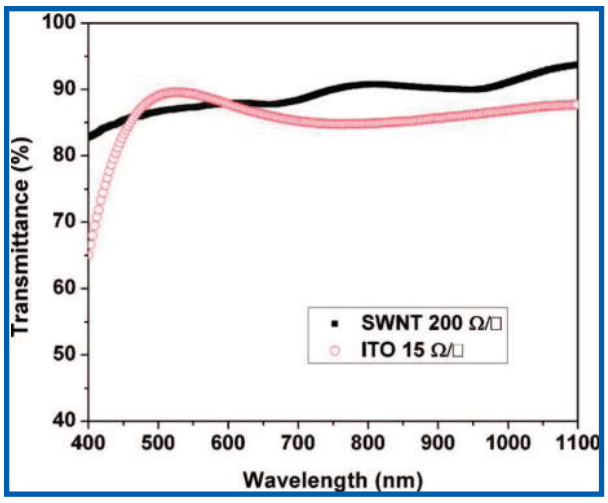


**Figure 13.** Transparency of a 30-nm-thick nanotube contact layer compared with the transparency of ITO on glass. (Reprinted with permission from ref 143. Copyright 2006 American Institute of Physics.)

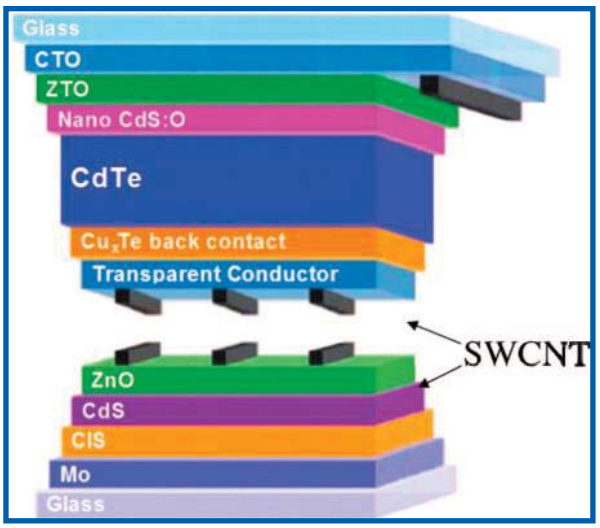


**Figure 14.** Structure of the NREL CdTe device with the NTN contact. (Courtesy Dr. Teresa M. Barnes, NREL.)

Shortly thereafter, two reports demonstrated new methods for making highly uniform improved nanotube contact layers. For example, conductive coatings were made by layer-by-layer (LBL) assembly of SWNTs. These films had electrical conductivities of $10^2$ to $\sim 10^3$ S/m at room temperature, with the nanotube loading as low as ~10%. This thus indicated an efficient utilization of SWNT percolation pathways.[146] In 2009, polymer-assisted direct deposition was demonstrated for uniform carbon nanotube networks for high performance transparent electrodes.[147] In this report, the addition of small amounts of a conjugated polymer to nanotube dispersions

enabled straightforward fabrication of uniform NTNs by spin-coating. The technique also allowed for simultaneous tuning of parameters such as bundle size and density, enabling the nanotube content to be minimized. These NTNs had sheet resistances competitive with those of the other reported carbon nanotube based transparent electrodes.[147] Also, a nanocomposite transparent film comprised of graphene and SWNTs was demonstrated to have a sheet resistance of 240 Ω/square with 86% transmittance.[148] Finally, in 2009, R. C. Tenent et al. reported a simple spray deposition process for depositing SWNT transparent contacts with a sheet resistance of 60 Ω/square.[149] The spray deposition processing could be employed in roll-to-roll manufacturing technologies for the fabrication of large-area devices.[149]

### 3. Nanotubes for Electrical Energy Storage Devices

Improvements in both batteries and electrochemical capacitors will enable the next-generation of electric vehicles and could also impact stationary electrical energy storage. Electrochemical capacitors have unusually high energy densities when compared to common capacitors as well as very high specific short duration peak power (i.e., rapid energy delivery). Batteries have significantly higher energy densities than electrochemical capacitors with lower short duration peak power. For example, Li-ion batteries have specific energy densities of hundreds of (W h)/kg with electrochemical capacitors having specific energy densities ranging from several to tens of (W h)/kg. However, the short duration peak power of an electrochemical capacitor exceeds 1000 W/kg, which is an order of magnitude better than that of typical Li-ion batteries. Carbon nanotubes may be employed to improve both of these technologies, as reviewed in detail below. In general, the utilization of carbon nanotubes for electrical energy storage remains the subject of relatively fundamental research. However, carbon MWNTs may be produced at a level of ∼400 tons/year commercially and subsequently employed as additives to stabilize Li-ion battery electrodes.[150]

#### 3.1. Li-Ion Batteries

Lithium-ion batteries are the current power sources of choice for portable electronics, offering high energy density and longer lifespan than comparable technologies.[23,151,152] Furthermore, Li-ion technologies have sufficient specific energy and power densities to meet the U.S. DOE targets for hybrid electric vehicles and plug-in hybrid electric vehicles for up to a 40-mile battery range.[153] However, significant improvements in durability, especially at high rate, for inexpensive, safe, and nontoxic electrode materials, are still warranted before Li-ion batteries are employed for large-scale application in the transportation sector. Increasing the specific capacities of electrode materials will also enable an extended battery range for PHEVs.[149] There are several recent reviews of battery materials that have been the focus of ongoing research efforts.[21,151,154] Here the potential for carbon nanotubes to improve state-of-the-art Li-ion batteries for possible deployment in next-generation electric vehicles is discussed in detail.

In general, carbon nanotubes are employed to improve Li-ion anodes, as the commercially employed anode is typically graphite (with some similar properties to CNTs). The specific capacity of graphite in most commercial batteries is ∼350 (mA h)/g (gravimetric) and ∼770 (mA h)/cm$^3$ (volumetric). Graphite is very durable, showing little capacity fade over hundreds of charge/discharge cycles, and it operates at a potential of ∼0.1 V versus $Li^+$/Li. However, recent efforts for hybrid electric vehicle applications have been focused on new anode materials with slightly more positive insertion voltages with respect to $Li^+$/Li to minimize any risks of high-surface-area Li plating while charging at high rates, a major safety concern.[155] In hybrid electric vehicles, batteries are cycled with ∼10% charge/discharge from the point where the cell is at 50% capacity.[156] Thus, the ideal negative electrode for forthcoming vehicular applications may have a charge/discharge potential of ∼0.5 V vs $Li^+$/Li when it is approximately one-half charged. Consequently, transition metal oxides[157−160] that operate at higher potential than that of graphite are under consideration for next generation anode technologies.

In a detailed study in 2003, nanocomposites of MWNTs with Sb and SnSb particles were prepared by chemical reduction of $SnCl_2$ and SbCl precursors in the presence of MWNTs.[161] The MWNT−metal composites were then demonstrated as active anode materials for Li-ion batteries, showing improved cycling capability compared to unsupported Sb and Sn−Sb particles and also higher reversible specific capacities than MWNTs alone. The reversible capacities were as high as 462 (mA h)/g for MWNT/36 wt % Sb and 518 (mA h)/g for MWNT/56 wt % SnSb. After 30 cycles, the capacity was 62.1% of the initial capacity for the former and 67.2% of the initial capacity for the later. In comparison, Sb and SnSb could only retain 17.7 and 23.5%, respectively, of their initial capacities in the same number of cycles. The improvement in cycling durability was attributed to the nanodimension of the metal particles and the MWNTs relieving mechanical stress induced by volume changes that occur upon $Li^+$ insertion and extraction.[161] Also in 2003, a carbon nanotube coated Cr-doped Si anode was shown to have superior cycling performance than the uncoated Cr-doped Si.[162] In the optimized electrode, the anode had a capacity of ∼1500 (mA h)/g that was sustained for ten cycles. Shortly thereafter, SWNT/Nafion composites were prepared with a simple chemical dispersion technique and then shown to be promising for electrochemical applications.[163]

In a very creative report, published in 2007, the design and fabrication of flexible MWNT−cellulose−room temperature ionic liquid (RTIL) nanocomposite sheets, that could be employed as flexible, Li-ion batteries, ultracapacitors, and/or hybrids of the two, was demonstrated.[164] Figure 15 is a schematic representation of the design fabrication of the nanocomposite paper units for both the ultracapacitor and battery. In Figure 15 a), it is shown that the ultracapacitor and battery are assembled by using nanocomposite film units. The nanocomposite unit comprises both RTIL and MWNTs embedded inside a cellulose paper. A thin layer of cellulose then covers the top of the MWNT array. Ti/Au thin films were then deposited on the exposed MWNTs to provide a current collector. In the battery, a thin lithium metal electrode served as the counter electrode. Figure 15b displays photographs of the nanocomposites, and part c displays a cross-sectional SEM image of the nanocomposite paper showing MWNTs protruding from the cellulose−RTIL thin films, with a schematic also displaying the partial exposure of MWNTs from the flexible device.[164]

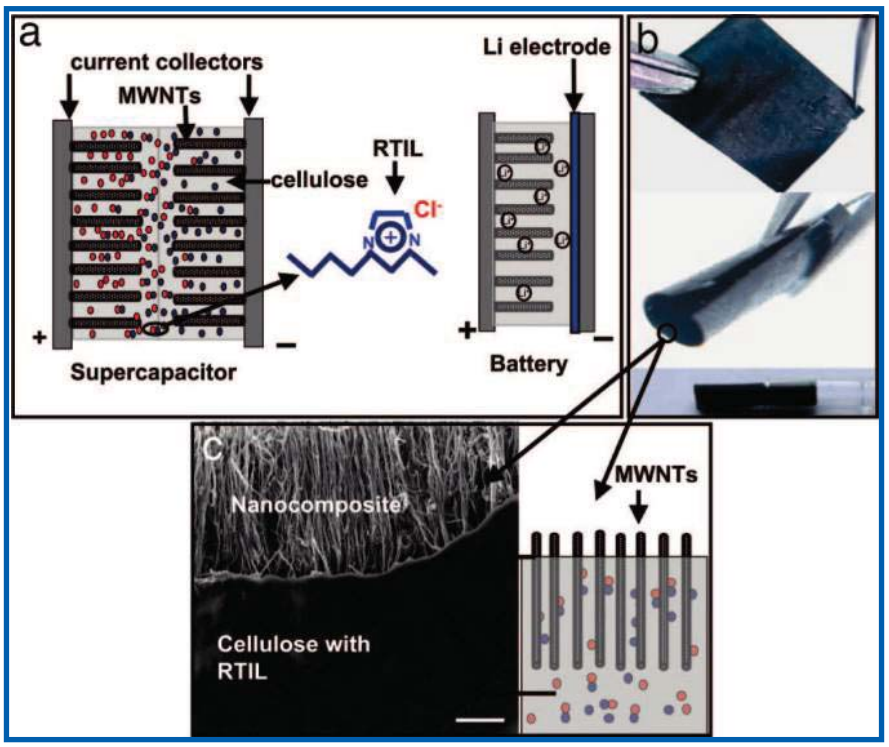


**Figure 15.** Schematic representation of the fabrication of the nanocomposite paper units for supercapacitor and battery. (a) The supercapacitor and battery assembled by using nanocomposite film units. The nanocomposite unit comprises RTIL and MWNTs embedded inside cellulose paper. A thin extra layer of cellulose covers the top of the MWNT array. The Ti/Au thin film deposited on the exposed MWNT acts as a current collector. In the battery, a thin Li electrode is added to the nanocomposite. (b) Photographs of the nanocomposite units demonstrating mechanical flexibility. Flat sheet (top), partially rolled sheet (middle), and completely rolled up sheet inside a capillary (bottom) are shown and (c) cross-sectional SEM image of the nanocomposite paper showing MWNTs protruding from the cellulose-RTIL thin films. (Scale bar, 2 $\mu$m.) The schematic displays the partial exposure of MWNTs. (Reprinted with permission from ref 152. Copyright 2007 National Academy of Sciences.)

In 2009 the Li-ion storage properties of SWNT pea pods containing one of three organic molecules (9,10-dichloroanthracene, $\beta$-carotene, coronene) were measured.[165] (CNT pea pods are nanotubes with encapsulated $C_{60}$ molecules discovered by D. L. Luzzi, VOM in 1998[166]). It was found that the reversible Li-ion capacity of the SWNT pea pods significantly increased as a result of the inclusion of the organic molecules. Unfortunately, the new anode material was not demonstrated as a useful candidate for Li-ion batteries because of a high initial irreversible capacity (>900 (mA h)/g).[165] Also in 2009, in an unusual example, MWNT arrays coated with $MnO_2$ were demonstrated as a potential new cathode material for Li-ion batteries.[167]

Finally, in a seminal report by C. Ban et al., an improved anode technology was demonstrated by combining $Fe_3O_4$ nanorods as the active material for lithium storage and carbon SWNTs as the conductive additive. The SWNTs improved both mechanical integrity and electrical conductivity as well as enabled a high volumetric energy density to be achieved. The highest reversible capacity was obtained using only 5 wt % SWNTs. The reversible capacity of the anode when coupled with a lithium metal electrode reached 1000 (mA h)/g at rate *C* (one charge/discharge in one hour), which was sustained over 100 cycles with a volumetric capacity of ~2000 (mA h)/cm.[168] Furthermore, a high rate capability and a stable capacity of 800 (mA h)/g at 5*C* (one charge/discharge in 12 min) and a stable capacity of ~600 (mA h)/g at 10*C* (one charge/discharge in 6 min) were demonstrated. Scanning electron microscopy revealed that the $Fe_3O_4$ nanorods were uniformly suspended in the conductive matrix of SWNTs, allowing for the improved rate capability and durability of the high volume expansion iron oxide structures. Figure 16 displays (a) an SEM image of the $Fe_3O_4$ nanorod/SWNT electrode. Note, the $Fe_3O_4$ nanorods, with an average width of 100 nm, are dispersed with a regular pore structure. In Figure 16b a color enhanced cross-sectional image also shows that small bundles of SWNTs are interlaced with the $Fe_3O_4$ nanorods and that the $Fe_3O_4$ nanorods are uniformly suspended in the SWNT conductive matrix.[168]

## 3.2. Electrochemical Capacitors

Electrochemical capacitors store significantly less energy than batteries but are capable of very rapid charge and discharge, making them promising for both stationary and automotive applications. Depending on the charge storage mechanism, they are classified into two types: electric double-layer capacitors based on carbon electrodes that house electrostatic charge, and pseodocapacitors that employ a material such as a metal oxide that undergoes Faradaic redox reactions to enable the charge storage. Since this review is focused on CNTs, the discussion will be limited to double-layer carbon electrochemical capacitors unless pseudocapacitance is induced by functionalization of the nanotubes themselves (rather than via direct incorporation of other pseudocapacitance materials).

In 2000,[169] the electrochemical capacitance behavior of MWNT electrodes was extensively explored as well as correlated with the microtexture and elemental composition of the materials. It was shown that the presence of mesopores due to the central canal allowed for easy accessibility of ions to the electrode/electrolyte interface and charging the electrical double layer. Pseudofaradaic reactions were detected upon oxidation of the MWNTs and varying the surface functional-

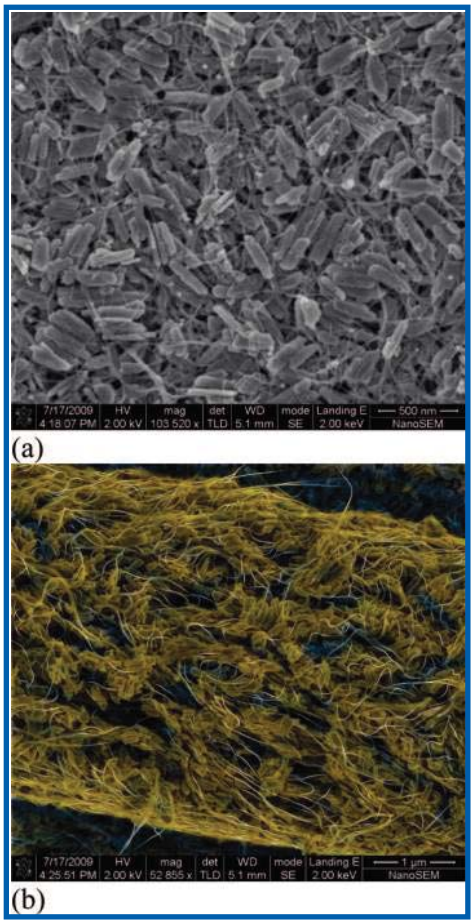


**Figure 16.** SEM micrographs of the nano $Fe_3O_4$ electrode: (a) surface and (b) cross section with colorization for effect. (Reprinted with permission from ref 168. Copyright 2010 Wiley-VCH Verlag GmbH & Co. KGaA.)

ity. The values of specific capacitance varied from 4 to 135 F/g, depending on the MWNT synthesis parameters and subsequent post-treatments, with the higher value only achieved when Faradaic reactions were observed.[169] Shortly thereafter, arc-generated SWNTs were reported to display a maximum specific capacitance of 180 F/g, a large power density of 20 kW/kg, and an energy density of 6.5 (W h)/kg. A heat treatment at 1000 °C was required to increase the capacitance and reduce the SWNT-electrode resistance. The increased capacitance was attributed to an increase in specific surface area of the SWNTs.[170]

Significantly later in 2005, an elegant method for spinning solid and hollow carbon nanotube fibers was reported.[171] The technique could be applied to either MWNTs or SWNTs. The SWNT fibers were shown to have a high electrochemical capacitance of ~100 F/g. Shortly thereafter in 2006, MWNT thin films were fabricated from an electrophoretic deposition technique. The thin films were demonstrated as electrochemical capacitors. Importantly, the thin films enabled very high rate capability to be achieved.[172] However, again heat treatment and functionalization suggested that Faradic reactions also contributed to the high capacitance and a specific power density of 20 kW/kg. In an additional study, by incorporating carbon MWNTs with activated carbon based electrodes for electrochemical capacitors, it was shown that the resistance of the electrodes could be decreased.[173] The optimized composite contained 15 wt % of carbon MWNTs laminated on an aluminum current collector. This composition in a two electrode 4 $cm^2$ cell had a specific capacitance of 88 F/g with a sheet resistance of only 600 m$\Omega$ $cm^2$.

In another seminal 2006 publication, a simple method to fabricate densely packed and aligned single-wall carbon nanotubes was demonstrated.[174] Aligned forests of SWNTs were initially grown with water assisted CVD.[175] However, the forests had a typical mass density of only 0.03 g $cm^{-3}$, with an average diameter of ~2.8 nm and a very significant fraction of empty space (~97%).[176] By "dropping" various liquids, including both water and organic solvents, on the forests, it was possible to make the as-grown SWNT forests significantly denser. This packing was speculated to occur in two steps: liquid immersion and subsequent evaporation. In the first step, the tubes were drawn together through liquid capillary forces. Then upon evaporation, van der Waals forces caused the tubes to further agglomerate and form a rigid single body, as depicted in Figure 17a, where a 1 × 1 $cm^2$ as-grown SWNT forest was contacted with a drop of water in the middle and allowed to dry (schematic representation shown in Figure 17b. The liquid-induced collapse resulted in a 4.5-fold decrease in the two lateral dimensions but no detectable change in the height, producing an ≈20-fold increase in mass density (Figure 17c). Furthermore, the forest densification action proceeded without damaging the tubes, as demonstrated by the almost identical Raman spectra in Figure 1d before and after the liquid initiated collapse. Additional characterization also revealed that the SWNTs are densely packed. Scanning electron microscope images of the initial forest (Figure 17e) and collapsed forest (Figure 17f) surfaces (side-view) revealed a marked increase in the nanotube density following collapse. In fact, atomic force microscopy imaging revealed a smooth and highly uniform surface without significant gaps in the microstructure (Figure 1g). The double layer electrochemical capacitance of the *dense* SWNT forests was found to be 80 F/g for a three electrode cell.[174]

In 2007, tubes-in-tube MWNTs consisting of outer nanotubes with an average diameter of 50 nm and inner nanotubes with diameters in the range 3−10 nm were shown to have an average capacitance of 203 F/g. The very high capacitance was again achieved by both electrostatic attraction in the double layer and a Faradic reaction caused by the existence of OH functional groups on the MWNTs.[177] In 2008, MWNTs were grown on or "grafted to" activated carbon fibers that were employed as an electrode for electric double layer capacitors.[178] The nanotubes were grown by first employing sputter deposition to deposit Ni catalyst particles on the carbon fiber surface and subsequent CVD deposition. A capacitor cell assembled with the MWNT-grafted fibers showed higher electron and electrolyte-ion conductivities relative to a cell assembled with only the bare carbon fibers. Furthermore, the MWNT containing electrodes maintained a significantly higher capacitance when the discharge current density was increased from 1 to 150 mA/$cm.^2$ The same group also reported that grafted MWNTs could enhance the power capability of carbon cloths when tested as electric double layer capacitors.[179] The carbon cloth was a simple commercially available polyacrylonitrile-based activated carbon, purchased from Taiwan Carbon Technology Co. Again, a decrease in capacitance loss was observed for the MWNT-grafted cloth for a current density as high as 150 mA/$cm.^2$

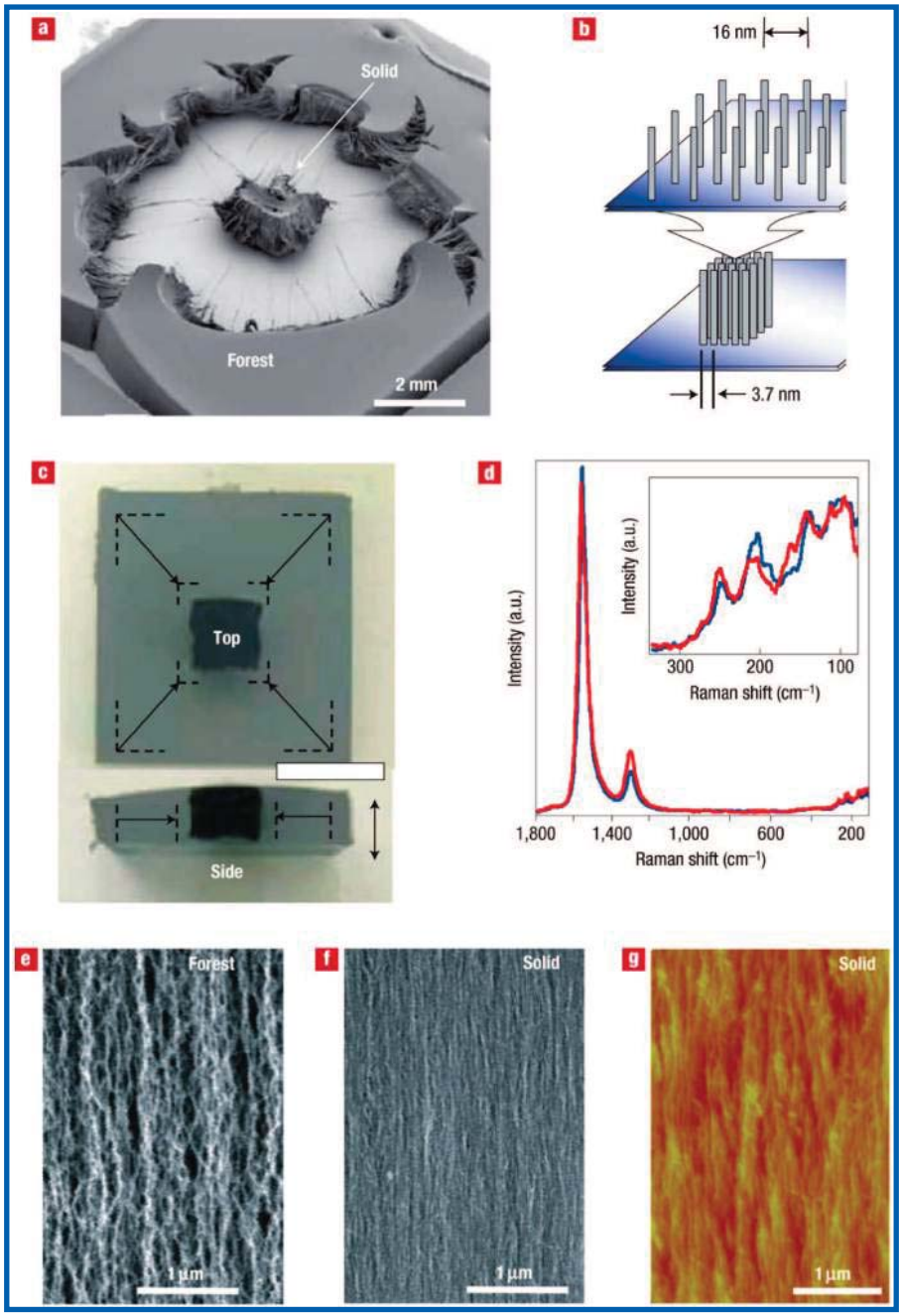


**Figure 17.** Liquid-induced collapse of SWNT forests: (a) SEM image of SWNT-forest structural collapse from a single drop of water. (b) Schematic diagram of the collapse of the aligned low-density as-grown forest to the highly densely packed SWNT solid. (c) Overlaid images illustrating a decrease in lateral dimensions before (gray) and after (black) collapse. The double-ended arrow indicates the tube alignment direction, and the scale bar is 1 cm. (d) Raman spectra for the as-grown forest (blue) and SWNT collapsed forest (red). SEM images of the as-grown forest (e) and the collapsed forest (f). (g) Atomic force microscope image of collapsed surface. (Reprinted with permission from ref 174. Copyright 2006 Nature Materials.)

## 4. Conclusions and Future Directions

The highly unique physical properties of carbon nanotubes have been demonstrated for a variety of photovoltaic devices as well as improved Li-ion batteries and electrochemical capacitors. For example, nanotubes have been matched with an inorganic layer to create heterojunction solar cells. An optimized hybrid approach resulted in monochromatic power-conversion efficiencies of up to 10.7% for a MWNT/pyrene$^{+}$/ZnP$^{8-}$ stack.[100] Carbon nanotubes have also been employed in PV devices to improve both exciton generation as well as transport of photoexcited carriers. T. Hasobe et al. reported the construction of photochemical solar cells from assemblies of SWNTs and protonated porphyrin on nanostructured $SnO_2$ electrodes.[105] The organized assemblies were shown to be photoactive, absorbing strongly at visible wavelengths with an incident photon to photocurrent efficiency of 13%. The power conversion efficiency for this MWNT/ZnO quantum dot system was measured to be above 1%.[109] In many instances nanotubes have been demonstrated as either electron donors or acceptors in novel organic photovoltaic technologies. In 2007, an OPV device was fabricated with a P3HT/PCBM (1:1) mixture with 0.1 wt % MWNTs. This optimized cell had a $V_{oc}$ of 0.57 V, an $J_{sc}$ of 9.3 mA cm$^{-2}$, and a fill factor of 0.384, which lead to a conversion efficiency of 2.0%.[124] Finally, very thin transparent films of nanotubes have been explored as transparent conducting

contact layers for a variety of PV or other optoelectronic devices. In 2009, R. C. Tenent et al. reported a simple spray deposition process for depositing SWNT transparent contacts with a sheet resistance of 60 Ω/square.[149] The spray deposition processing could be employed in roll-to-roll manufacturing technologies for the fabrication of large-area devices.[149] Finally, SWNTs were employed to demonstrate a potential new anode for Li-ion batteries for vehicular applications. The reversible capacity of the anode when coupled with a lithium metal electrode reached 1000 (mA h)/g at rate *C* (one charge/discharge in one hour) that was sustained over 100 cycles with a volumetric capacity of ∼2000 (mA h)/cm.[168] A very dense SWNT forest has also been elegantly demonstrated for electrochemical capacitor applications.[174]

Thus, it is apparent that CNTs are promising candidates for both PV and electrical energy storage technologies. It is also clear that utilizing nanotubes in either of these technologies is a relatively new endeavor, indicating that future research efforts will be abundant. It is, however, especially important to consider that the fabrication of crystalline graphitic MWNTs that are easily purified has been demonstrated with cost-effective methods that are commercially scalable. In contrast, the fabrication of crystalline graphitic SWNTs that are easily purified is generally only achieved when the nanotubes are fabricated with laser vaporization. The applications presented here for SWNTs that are the closest to commercialization are most likely represented by the possible employment of SWNTs as transparent conducting contacts for PV or other devices as well as the utilization of SWNTs as a conductive additive in Li-ion battery applications. It is noted that, in this article, the highest quality transparent conducting contact[149] as well as the most impressive demonstration of SWNTs as a conductive additive in Li-ion batteries[168] was achieved with laser-generated SWNTs. It thus seems that efforts to make laser vaporization an industrially scalable technique and/or the demonstration of improved CVD technologies are needed.

Recently, countries including France, Germany, and Japan have devoted national efforts to scale the production of laser vaporization-SWNTs to manufacturing levels. Typical diode-pumped industrial lasers, routinely used in factories, for laser welding and cutting can continuously supply 4.5 kW of laser output and run around the clock. A simple linear scaling implies rates of ∼100 g/h. The most inexpensive carbon sources may be used, so estimating an initial cost of $500K for the laser, an annual operating cost of $50K, and a power efficiency of 10% yields nonlabor costs of approximately $16/h or $160/kg. While current laser vaporization technologies utilize solid carbon targets, heat losses due to thermal conduction decrease the vaporization rates significantly. The use of powders as targets could solve this problem. Moreover, the powder vaporization approach could greatly enhance the efficiency of the process and cut laser SWNT production costs more. Literature values indicate 20 g/100 W/h vaporization of micrometer-sized powders with theoretical limits of 100 g/100 W/h.[180] These rates suggest that an industrial laser with a powder feedstock could cut laser-generated SWNTs to a cost of ∼$3.20 per kilogram. These simple calculations therefore imply that the U.S. should fund the scale-up of laser-generated SWNTs at a significant level.

Other forms of nanographitic carbons may also prove promising in the development of next-generation renewable energy devices. For example, graphene, which consists of a single sheet of graphite, has been touted as an especially promising form of carbon for device engineering applications.[181] There is also already a significant volume of literature devoted to graphene and other forms of carbon including graphitic nanofibers that suggest that CNTs are not the only promising nanostructures for both photoconversion and electrical energy storage applications. This work, however, remains outside the scope of the current review.

## 5. Abbreviations

| | |
|---|---|
| CNTs | carbon nanotubes |
| C | rate one charge/discharge in one hour |
| CVD | chemical vapor deposition |
| DOE | Department of Energy |
| DWNTs | double-wall nanotubes |
| HEVs | hybrid electric vehicles |
| HiPCO | high-pressure carbon monoxide |
| $J_{sc}$ | short circuit current density |
| ITO | indium tin oxide |
| M | metallic |
| MWNTs | multiwall nanotubes |
| NREL | National Renewable Energy Laboratory |
| NTN | nanotube network |
| OPV | organic photovoltaic |
| P3HT | regioregularpoly(3-hexylthiophene) |
| PCBM | fullerene derivative 1-(3-methoxycarbonyl propyl-1-phenyl[6,6]$C_{61}$ |
| PHEVs | plug-in hybrid electric vehicles |
| PV | photovoltaics |
| RTIL | room temperature ionic liquid |
| S | semiconducting |
| SEM | scanning electron microscope |
| SWNTs | single-wall nanotubes |
| VOM | vision in own mind |
| $V_{oc}$ | open circuit voltage |
| TEM | transmission electron microscope |
| TCO | transparent conducting oxide |
| U.S. | United States |

## 6. Acknowledgments

This work was funded by the U.S. Department of Energy under subcontract number DE-AC36-08GO28308 through the DOE Office of Energy Efficiency and the Renewable Energy Office of the Vehicle Technologies Program and NREL's Laboratory Directed Research and Development Program. I would like to thank R. P. Mirin at the National Institute of Standards and Technology, D. B. Geohegan at Oak Ridge National Laboratory, and T. M. Barnes at NREL for useful discussions. Finally, I would like to express my deepest thanks to S. E. Asher for enabling my career at NREL.

## 7. References

(1) In http://www1.eere.energy.gov/solar/photovoltaics.html; Energy Efficiency and Renewable Energy, Solar Energy Technologies Program, 2009.
(2) Inhttp://www1.eere.energy.gov/vehiclesandfuels/about/partnerships/freedomcar/index.html; Energy Efficiency and Renewable Energy, Office of Vehicle Technologies, 2009.
(3) In http://www.er.doe.gov/bes/reports/abstracts.html#EES; Basic Energy Sciences, 2008.
(4) Iijima, S. *Nature* **1991**, *354*, 56.
(5) Dillon, A. C.; Yudasaka, M.; Dresselhaus, M. S. J. *Nanosci. Nanotechnol.* **2004**, *407*, 691.
(6) Avouris, P. *MRS Bull.* **2004**, *29*, 403.
(7) Jorio, A.; Dresselhaus, G.; Dresselhaus, M. S. *Carbon Nanotubes: advanced topics in sythesis, structure and properties*; Springer: New York, 2007.

(8) Dillon, A. C.; Jones, K. M.; Bekkedahl, T. A.; Kiang, C. H.; Bethune, D. S.; Heben, M. J. *Nature* **1997**, *386*, 377.
(9) Dillon, A. C.; Mahan, A. H.; Alleman, J. L.; Heben, M. J.; Parilla, P. A.; Jones, K. M. *Thin Solid Films* **2003**, *430*, 292.
(10) Lehman, J. H.; Engtrakul, C.; Gennett, T.; Dillon, A. C. *Appl. Opt.* **2005**, *44*, 483.
(11) Lehman, J. H.; Deshpande, R.; Rice, P.; Dillon, A. C. *IR Phys.* **2006**, *47*, 246.
(12) Dillon, A. C.; Heben, M. *J. Appl. Phys. A: Mater. Sci. Process.* **2001**, *72*, 133.
(13) Dillon, A. C.; Mahan, A. H.; Deshpande, R.; Alleman, J. L.; Blackburn, J. L.; Parillia, P. A.; Heben, M. J.; Engtrakul, C.; Gilbert, K. E. H.; Jones, K. M.; To, R.; Lee, S. H.; Lehman, J. H. *Thin Solid Films* **2006**, *501*, 216.
(14) In http://www.eia.doe.gov/fueloverview.html.
(15) Dillon, A. C.; Nelson, B. P.; Zhao, Y.; Kim, Y.-H.; Tracy, C. E.; Zhang, S. B. *Materials Research Society Symposium Proceedings*; Materials Research Society: Boston, 2005.
(16) Lewis, N. http://www.its.caltech.edu/∼mmrc/nsl/energy.html.
(17) Ohi, J. J. *Mater. Res.* (Focus Issue), in press.
(18) Denholm, P.; Margolis, R. M. *Energy Policy* **2007**, *35*, 2852.
(19) Denholm, P.; Margolis, R. M. *Energy Policy* **2007**, *35*, 4424.
(20) Denholm, P.; Kulcinski, G. L.; Holloway, T. *Environ. Sci. Technol.* **2005**, *39*, 1903.
(21) Whittingham, M. S. *Chem. Rev.* **2004**, *104*, 4271.
(22) Chernova, N. A.; Roppolo, M.; Dillon, A. C.; Whittingham, M. S. *J. Mater. Chem.* **2009**, *19*, 2526.
(23) Lee, S.-H.; Kim, Y.-H.; Deshpande, R.; Parilla, P. A.; Whitney, E.; Gillaspie, D. T.; Jones, K. M.; Mahan, A. H.; Zhang, S. B.; Dillon, A. C. *Adv. Mater.* **2008**, *20*, 3627.
(24) Iijima, S.; Ichihashi, T. *Nature* **1993**, *363*, 603.
(25) Bethune, D. S.; Kiang, C.-H.; Vries, M. S. d.; Gorman, G.; Savoy, R.; Vasquez, J.; Beyers, R. *Nature* **1993**, *363*, 605.
(26) Dresselhaus, M. S.; Dresselhaus, G.; Saito, R. *Solid State Commun.* **1992**, *84*, 201.
(27) Journet, C.; Maser, W. K.; Bernier, P.; Loiseau, A.; Lamy de la Chapells, M.; Lefrant, S.; Deniard, P.; Lee, R.; Fischer, J. E. *Nature* **1997**, *388*, 756.
(28) Bandow, S. Private communication.
(29) Guo, T.; Nikolaev, P.; Thess, A.; Colbert, D. T.; Smalley, R. E. *Chem. Phys. Lett.* **1995**, *243*, 49.
(30) Thess, A.; Lee, R.; Nikolaev, P.; Dai, H.; Pitit, P.; Robert, J.; Xu, C.; Lee, Y. H.; Kim, S. G.; Rinzler, A. G.; Colbert, D. T.; Scuseria, G. E.; Tomanek, D.; Fischer, J. E.; Smalley, R. E. *Science* **1996**, *273*, 483.
(31) Heben, M. J.; Dillon, A. C.; Gilbert, K. E. H.; Parilla, P. A.; Gennett, T.; Alleman, J. L.; Hornyak, G. L.; Jones, K. M. *Hydrogen Mater. Vac. Syst.* **2002**, *671*, 77.
(32) Dillon, A. C.; Parilla, P. A.; Alleman, J. L.; Gennett, T.; Jones, K. M.; Heben, M. J. *Chem. Phys. Lett.* **2005**, *401*, 522.
(33) Kataura, H.; Maniwa, Y.; Abe, M.; Fujiwara, A.; Kodama, T.; Kikuchi, K.; Imahori, H.; Misaki, Y.; Suzuki, S.; Achiba, Y. *Appl. Phys. A: Mater. Sci. Process.* **2002**, *74*, 349.
(34) Dillon, A. C.; Gennett, T.; Jones, K. M.; Alleman, J. L.; Parilla, P. A.; Heben, M. J. *Adv. Mater.* **1999**, *11*, 1354.
(35) Dai, H.; Rinzler, A. G.; Nikolaev, P.; Thess, A.; Colbert, D. T.; Smalley, R. E. *Chem. Phys. Lett.* **1996**, *260*, 471.
(36) Peigney, A.; Laurent, C.; Dobigeon, F.; Rousset, A. *J. Mater. Res.* **1997**, *12*, 613.
(37) Hafner, J. H.; Bronikowski, M. J.; Azamian, B. R.; Nikolev, P.; Rinzler, A. G.; Colbert, D. T.; Smith, K. A.; Smalley, R. E. *Chem. Phys. Lett.* **1998**, *296*, 195.
(38) Cheng, H. M.; Li, F.; Su, G.; Pan, H. Y.; He, L. L.; Sun, X.; Dresselhaus, M. S. *Appl. Phys. Lett.* **1998**, *72*, 3282.
(39) Cassell, A. M.; Raymakers, J. A.; Kong, J.; Dai, H. *J. Phys. Chem. B* **1999**, *103*, 6484.
(40) Colomer, J.-F.; Stephan, C.; Lefrant, S.; Van Tendeloo, G.; Willems, I.; Konya, Z.; Fonseca, A.; Laurent, C.; Nagy, J. B. *Chem. Phys. Lett.* **2000**, *317*, 83.
(41) Su, M.; Zheng, B.; Liu, J. *Chem. Phys. Lett.* **2000**, *322*, 321.
(42) Bronikowski, M. J.; Willis, P. A.; Colbert, D. T.; Smith, K. A.; Smalley, R. E. *J. Vac. Sci. Technol. A* **2001**, *19*, 1800.
(43) Li, Q.; Hao, Y.; Yan, C.; Jin, Z.; Liu, Z. J. *Mater. Chem.* **2002**, *12*, 1179.
(44) Hornyak, G. L.; Grigorian, L.; Dillon, A. C.; Parilla, P. A.; Jones, K. M.; Heben, M. J. *J. Phys. Chem. B* **2002**, *106*, 2821.
(45) Wagg, L. M.; Hornyak, G. L.; Grigorian, L.; Dillon, A. C.; Jones, K. M.; Blackburn, J.; Parilla, P. A.; Heben, M. J. *J. Phys. Chem. B* **2005**, *109*, 10435.
(46) Hafner, J. H.; Cheung, C.-L.; Oosterkamp, T. H.; Lieber, C. M. *J. Phys. Chem. B* **2001**, *105*, 743.
(47) Mahan, A. H.; Alleman, J. L.; Heben, M. J.; Parilla, P. A.; Jones, K. M.; Dillon, A. C. *Appl. Phys. Lett.* **2002**, *81*, 4061.
(48) Chiang, I. W.; Brinson, B. E.; Huang, A. Y.; Willis, P. A.; Bronikowski, M. J.; Margrave, J. L.; Smalley, R. E.; Hauge, R. H. *J. Phys. Chem. B* **2001**, *105*, 8297.
(49) Hurst, K. E.; Dillon, A. C.; Yang, S.; Lehman, J. H. *J. Phys. Chem. C* **2008**, *112*, 16296.
(50) Chattopadhyay, D.; Galeska, I.; Papadimitrakopoulos, F. *J. Am. Chem. Soc.* **2003**, *125*, 3370.
(51) Zheng, M.; Jagota, A.; Semke, E. D.; Diner, B. A.; McLean, R. S.; Lustig, S. R.; Richardson, R. E.; Tassi, N. G. *Nat. Mater.* **2003**, *2*, 338.
(52) Hersam, M. C. *Nature* **2009**, *460*, 186.
(53) Krupke, R.; Hennrich, F.; Lohneysen, H. v.; Kappes, M. M. *Science* **2003**, *301*, 344.
(54) Arnold, M. S.; Alexander, A. G.; Hulvat, J. F.; Stupp, S. I.; Hersam, M. C. *Nature Nanotechnol.* **2006**, *1*, 60.
(55) Tanaka, T.; Urabe, Y.; Nishide, D.; Kataura, H. *Appl. Phys. Express* **2009**, *2*, 3.
(56) Huang, H. J.; Kajiura, H.; Maruyama, R.; Kadono, K.; Noda, K. *J. Phys. Chem. B* **2006**, *110*, 4686.
(57) Ebbesen, T. W.; Ajayan, P. M. *Nature* **1992**, *358*, 220.
(58) Dillon, A. C.; Mahan, A. H.; Parilla, P. A.; Alleman, J. L.; Heben, M. J.; Jones, K. M.; Gilbert, K. E. H. *Nano Lett.* **2003**, *3*, 1425.
(59) Wang, W. D.; Serp, P.; Kalck, P.; Silva, C. G.; Faria, J. L. *Mater. Res. Bull.* **2008**, *43*, 958.
(60) Ribaya, B. P.; Leung, J.; Brown, P.; Rahman, M.; Nguyen, C. V. *Nanotechnology* **2008**, *19*.
(61) Bokobza, L. *Polymer* **2007**, *48*, 4907.
(62) Raffaelle, R. P.; Landi, B. J.; Harris, J. D.; Bailey, S. G.; Hepp, A. F. *Materials Science and Engineering B-Solid State Materials for Advanced Technology* **2005**, 233–243.
(63) Ngo, Q.; Petranovic, D.; Krishnan, S.; Cassell, A. M.; Ye, Q.; Li, J.; Meyyappan, M.; Yang, C. Y. *IEEE Trans. Nanotechnol.* **2004**, *3*, 311.
(64) Gong, K. P.; Zhang, M. N.; Yan, Y. M.; Su, L.; Mao, L. Q.; Xiong, Z. X.; Chen, Y. *Anal. Chem.* **2004**, *76*, 6500.
(65) Gomes, H. T.; Samant, P. V.; Serp, P.; Kalck, P.; Figueiredo, J. L.; Faria, J. L. *Appl. Catal., B* **2004**, *54*, 175.
(66) Lueking, A.; Yang, R. T. *J. Catal.* **2002**, *206*, 165.
(67) Qin, L. C. J. *Mater. Sci. Lett.* **1997**, *16*, 457.
(68) Fan, Y.-Y.; Li, F.; Cheng, H.-M.; Su, G.; Yu, Y.-D.; Shen, Z.-H. *J. Mater. Res.* **1998**, *13*, 2342.
(69) Marangoni, R.; Serp, P.; Feurer, R.; Kihn, Y.; Kalck, P.; Vahlas, C. *Carbon* **2001**, *39*, 443.
(70) Andrews, R.; Jacques, D.; Rao, A. M.; Derbyshire, F.; Qian, D.; Fan, X.; Dickey, E. C.; Chen, J. *Chem. Phys. Lett.* **1999**, *303*, 467.
(71) Endo, M.; Takeuchi, K.; Igarashi, S.; Kobori, K.; Shiraishi, M.; Kroto, H. W. J. *Phys. Chem. Sol.* **1993**, *54*, 1841.
(72) Jose-Yacaman, M.; Miki-Yoshida, M.; Rendon, L.; Santiesteban, J. G. *Appl. Phys. Lett.* **1993**, *62*, 202.
(73) Ivanov, V.; Nagy, J. B.; Lambin, P.; Lucas, A.; Zhang, X. B.; Zhang, X. F.; Bernaerts, D.; Van Tendeloo, G.; Amelinckx, S.; Van Landuyt, J. *Chem. Phys. Lett.* **1994**, *223*, 329.
(74) Thong, J. T. L.; Oon, C. H.; Eng, W. K.; Zhang, W. D.; Gan, L. M. *Appl. Phys. Lett.* **2001**, *79*, 2811.
(75) Tang, D. S.; Xie, S. S.; Pan, Z. W.; Sun, L. F.; Liu, Z. Q.; Zou, X. P.; Li, Y. B.; Ci, L. J.; Liu, W.; Zou, B. S.; Zhou, W. Y. *Chem. Phys. Lett.* **2002**, *356*, 563.
(76) Lee, C. J.; Kim, D. W.; Lee, T. J.; Choi, Y. C.; Park, Y. S.; Kim, W. S.; Lee, Y. H.; Choi, W. B.; Lee, N. S.; Kim, J. M.; Choi, Y. G.; Yu, S. C. *Appl. Phys. Lett.* **1999**, *75*, 1721.
(77) Xie, S.; Li, W.; Pan, Z.; Chang, B.; Sun, L. *Mater. Sci. Eng. A* **2000**, *286*, 11.
(78) Li, Y. J.; Sun, Z.; Lau, S. P.; Chen, G. Y.; Tay, B. K. *Appl. Phys. Lett.* **2001**, *79*, 1670.
(79) Qin, L. C.; Zhou, D.; Krauss, A. R.; Gruen, D. M. *Appl. Phys. Lett.* **1998**, *72*, 3437.
(80) Chen, M.; Chen, C.-M.; Chen, C.-F. *J. Mater. Sci.* **2002**, *37*, 3561.
(81) Choi, Y. C.; Bae, D. J.; Lee, Y. H.; Lee, B. S.; Park, G.-S.; Choi, W. B.; Lee, N. S.; Kim, J. M. *J. Vac. Sci. Technol. A* **2000**, *18*, 1864.
(82) Chung, S. J.; Lim, S. H.; Lee, C. H.; Jang, J. *Diamond Relat. Mater.* **2001**, *10*, 248.
(83) Ho, G. W.; Wee, A. T. S.; Lin, J.; Tiju, W. C. *Thin Solid Films* **2001**, *388*, 73.
(84) Wang, H.; Lin, J.; Huan, C. H. A.; Dong, P.; He, J.; Tang, S. H.; Eng, W. K.; Thong, T. L. *J. Appl. Surf. Sci.* **2001**, *181*, 248.
(85) Zhang, Q.; Yoon, S. F.; Ahn, J.; Gan, B.; Rusli; Yu, M.-B. *J. Mater. Res.* **2000**, *15*, 1749.
(86) Yoon, H. J.; Kang, H. S.; Shin, J. S.; Son, K. J.; Lee, C. H.; Kim, C. O.; Hong, J. P.; Cha, S. N.; Song, B. G.; Kim, J. M.; Lee, N. S. *Physica B* **2002**, *323*, 344.
(87) Woo, Y. S.; Jeon, D. Y.; Han, I. T.; Lee, N. S.; Jung, J. E.; Kim, j. M. *Diamond Relat. Mater.* **2002**, *11*, 59.

(88) Lee, H.; Kang, Y.-S.; Lee, P. S.; Lee, J.-Y. *J. Alloys Compd.* **2002**, *330*, 569.
(89) Bower, C.; Zhou, O.; Zhu, W.; Werder, D. J.; Jin, S. *Appl. Phys. Lett.* **2000**, *77*, 2767.
(90) Park, K. H.; Lee, K. M.; Choi, S.; Lee, S.; Koh, K. H. *J. Vac. Sci. Technol. B* **2001**, *19*, 946.
(91) Ono, T.; Miyashita, H.; Esashi, M. *Nanotechnology* **2002**, *13*, 62–64.
(92) Han, J.-h.; Moon, B.-S.; Yang, W. S.; Yoo, J.-B.; Park, C. Y. *Surf. Coat. Technol.* **2000**, *131*, 93.
(93) Ren, Z. F.; Huang, Z. P.; Xu, J. W.; Wang, J. H.; Bush, P.; Siegal, M. P.; Provincio, P. N. *Science* **1998**, *282*, 1105.
(94) Chen, C.-F.; Lin, C.-L.; Wang, C.-M. *Jpn. J. Appl. Phys.* **2002**, *41*, L67.
(95) Avouris, P.; Freitag, M.; Perebeinos, V. *Carbon-nanotube optoelectronics*; Springer-Verlag: 2008.
(96) Zhao, J. J.; Chen, X. S.; Xie, J. R. H. *Anal. Chim. Acta* **2006**, *568*, 161.
(97) Kislyuk, V. V.; Dimitriev, O. P. *J. Nanosci. Nanotechnol.* **2008**, *8*, 131.
(98) Anghel, C.; Derycke, V.; Filoramo, A.; Lenfant, S.; Giffard, B.; Vuillaume, D.; Bourgoin, J. P. *Nano Lett.* **2008**, *8*, 3619.
(99) Somani, S. P.; Somani, P. R.; Umeno, M.; Flahaut, E. *Appl. Phys. Lett.* **2006**, *89*, 223505.
(100) Sgobba, V.; Rahman, G. M. A.; Guldi, D. M.; Jux, N.; Campidelli, S.; Prato, M. *Adv. Mater.* **2006**, *18*, 2264.
(101) Hasobe, T.; Murata, H.; Kamat, P. V. *J. Phys. Chem. C* **2007**, *111*, 16626.
(102) Chitta, R.; Sandanayaka, A. S. D.; Schumacher, A. L.; D'Souza, L.; Araki, Y.; Ito, O.; D'Souza, F. *J. Phys. Chem. C* **2007**, *111*, 6947.
(103) Liu, M.; Lu, G. H.; Chen, J. H. *Nanotechnology* **2008**, *19*, 265705.
(104) Li, Z. R.; Kunets, V. P.; Saini, V.; Xu, Y.; Dervishi, E.; Salamo, G. J.; Biris, A. R.; Biris, A. S. *Appl. Phys. Lett.* **2008**, *93*, 243117.
(105) Hasobe, T.; Fukuzumi, S.; Kamat, P. V. *J. Phys. Chem. B* **2006**, *110*, 25477.
(106) Vietmeyer, F.; Seger, B.; Kamat, P. V. *Adv. Mater.* **2007**, *19*, 2935.
(107) Pradhan, B.; Batabyal, S. K.; Pal, A. J. *Appl. Phys. Lett.* **2006**, *88*, 093106.
(108) Landi, B. J.; Evans, C. M.; Worman, J. J.; Castro, S. L.; Bailey, S. G.; Raffaelle, R. P. *Mater. Lett.* **2006**, *60*, 3502.
(109) Li, F. S.; Cho, S. H.; Son, D. I.; Kim, T. W.; Lee, S. K.; Cho, Y. H.; Jin, S. H. *Appl. Phys. Lett.* **2009**, *94*, 111906.
(110) Wei, J. Q.; Jia, Y.; Shu, Q. K.; Gu, Z. Y.; Wang, K. L.; Zhuang, D. M.; Zhang, G.; Wang, Z. C.; Luo, J. B.; Cao, A. Y.; Wu, D. H. *Nano Lett.* **2007**, *7*, 2317.
(111) Flicker, J.; Ready, J. *J. Appl. Phys.* **2008**, 113110−1.
(112) Liu, Y.; Lu, S. X.; Panchapakesan, B. *Nanotechnology* **2009**, *20*, 035203.
(113) Li, Z. R.; Kunets, V. P.; Saini, V.; Xu, Y.; Dervishi, E.; Salamo, G. J.; Biris, A. R.; Biris, A. S. *ACS Nano* **2009**, *3*, 1407.
(114) Tang, C. W. *Appl. Phys. Lett.* **1986**, *48*, 183.
(115) Schon, J. H.; Kloc, C.; Bucher, E.; Batlogg, B. *Nature* **2000**, *403*, 408.
(116) Halls, J. J. M.; Walsh, C. A.; Greenham, N. C.; Marsegilia, E. A.; Friend, R. H.; Morratti, S. C.; Holmes, A. B. *Nature* **1995**, *376*, 498.
(117) Yu, G.; Gao, J.; Hummelen, J.; Wudl, F.; Heeger, A. J. *Science* **1995**, *270*, 1789.
(118) Sariciftci, N. S.; Smilowitz, L.; Heeger, A. J.; Wudl, F. *Science* **1992**, *258*, 1474.
(119) http://www.eetasia.com/ART_8800475629_765245_NT_332d9ea0.HTM.
(120) Padinger, F.; Rittberger, R. S.; Sariciftci, N. S. *Adv. Funct. Mater.* **2003**, *13*, 85.
(121) Green, M. A. *Physica E* **2002**, *14*, 65.
(122) Kymakis, E.; Alexandrou, I.; Amaratunga, G. A. J. *J. Appl. Phys.* **2003**, *93*, 1764.
(123) Miller, A. J.; Hatton, R. A.; Silva, S. R. P. *Appl. Phys. Lett.* **2006**, *89*, 133117.
(124) Berson, S.; de Bettignies, R.; Bailly, S.; Guillerez, S.; Jousselme, B. *Adv. Funct. Mater.* **2007**, *17*, 3363.
(125) Nogueira, A. F.; Lomba, B. S.; Soto-Oviedo, M. A.; Correia, C. R. D.; Corio, P.; Furtado, C. A.; Hummelgen, I. A. *J. Phys. Chem. C* **2007**, *111*, 18431.
(126) Li, C.; Chen, Y. H.; Wang, Y. B.; Iqbal, Z.; Chhowalla, M.; Mitra, S. *J. Mater. Chem.* **2007**, *17*, 2406.
(127) Reyes-Reyes, M.; Lopez-Sandoval, R.; Liu, J.; Carroll, D. L. *Sol. Energy Mater. Sol. Cells* **2007**, *91*, 1478.
(128) Nish, A.; Hwang, J. Y.; Doig, J.; Nicholas, R. J. *Nanotechnology* **2008**, *19*, 095603.
(129) Fanchini, G.; Miller, S.; Parekh, L. B.; Chhowalla, M. *Nano Lett.* **2008**, *8*, 2176.
(130) Lewis, B. G.; Paine, D. C. *MRS Bull.* **2000**, *25*, 22.
(131) Haxel, G. B.; Hedrick, J. B.; Orris, G. J. *U.S. Geol. Surv.* **2002**, 087-02.
(132) Zhuangchun, W.; Zhihong, C.; Xu, D.; Logan, J. M.; Sippel, J.; Nikolou, M.; Kamaras, K.; Reynolds, J. R.; Tanner, D. B.; Hebard, A. F.; Rinzler, A. G. *Science* **2004**, *305*, 1273.
(133) Zhang, M.; Fang, S.; Zakhidov, A. A.; Lee, S. B.; Aliev, A. E.; Williams, C. D.; Atkinson, K. R.; Baughman, R. H. *Science* **2005**, *309*, 1215.
(134) Ulbricht, R.; Lee, S. B.; Jiang, X. M.; Inoue, K.; Zhang, M.; Fang, S. L.; Baughman, R. H.; Zakhidov, A. A. *Sol. Energy Mater. Sol. Cells* **2007**, *91*, 416.
(135) Ulbricht, R.; Jiang, X.; Lee, S.; Inoue, K.; Zhang, M.; Fang, S.; Baughman, R.; Zakhidov, A. *Phys. Status Solidi B: Basic Solid State Phys.* **2006**, *243*, 3528.
(136) Hu, L.; Hecht, D. S.; Gruner, G. *Nano Lett.* **2004**, *4*, 2513.
(137) Chernova, N. A.; Roppolo, M.; Dillon, A. C.; Whittingham, M. S. *J. Mater. Chem.* **2009**, *19*, 2526.
(138) Lee, S.-H.; Deshpande, R.; Parilla, P. A.; Jones, K. M.; To, B.; Mahan, A. H.; Dillon, A. C. *Adv. Mater.* **2006**, *18*, 763.
(139) Deshpande, R.; Lee, S.-H.; Mahan, A. H.; Parilla, P. A.; Jones, K. M.; Norman, A. G.; To, B.; Blackburn, J. L.; Mitra, S.; Dillon, A. C. *Solid State Ionics* **2007**, *178*, 895.
(140) Deshpande, R.; Lee, S. H.; Mahan, A. H.; Parilla, P. A.; Jones, K. M.; Norman, A. G.; To, B.; Blackburn, J. L.; Mitra, S.; Dillon, A. C. *Solid State Ionics* **2007**, *178*, 895.
(141) Gruner, G. *J. Mater. Chem.* **2006**, *16*, 3533.
(142) van de Lagemaat, J.; Barnes, T. M.; Rumbles, G.; Shaheen, S. E.; Coutts, T. J.; Weeks, C.; Levitsky, I.; Peltola, J.; Glatkowski, P. *Appl. Phys. Lett.* **2006**, *88*, 233503.
(143) Rowell, M. W.; Topinka, M. A.; McGehee, M. D.; Prall, H. J.; Dennler, G.; Sariciftci, N. S.; Hu, L. B.; Gruner, G. *Appl. Phys. Lett.* **2006**, *88*, 233506.
(144) Barnes, T. M.; Wu, X.; Zhou, J.; Duda, A.; van de Lagemaat, J.; Coutts, T. J.; Weeks, C. L.; Britz, D. A.; Glatkowski, P. *Appl. Phys. Lett.* **2007**, *90*, 243503.
(145) Contreras, M. A.; Barnes, T.; van de Lagemaat, J.; Rumbles, G.; Coutts, T. J.; Weeks, C.; Glatkowski, P.; Levitsky, I.; Peltola, J.; Britz, D. A. *J. Phys. Chem. C* **2007**, *111*, 14045.
(146) Shim, B. S.; Tang, Z. Y.; Morabito, M. P.; Agarwal, A.; Hong, H. P.; Kotov, N. A. *Chem. Mater.* **2007**, *19*, 5467.
(147) Hellstrom, S. L.; Lee, H. W.; Bao, Z. N. *ACS Nano* **2009**, *3*, 1423.
(148) Tung, V. C.; Chen, L. M.; Allen, M. J.; Wassei, J. K.; Nelson, K.; Kaner, R. B.; Yang, Y. *Nano Lett.* **2009**, *9*, 1949.
(149) Tenent, R. C.; Barnes, T. M.; Bergeson, J. D.; Ferguson, A. J.; To, B.; Gedvilas, L. M.; Heben, M. J.; bBlackburn, J. L. *Adv. Mater.* **2009**, *21*, 1.
(150) http://www.sdk.co.jp/aa/english/news/2010/aanw_10_1224.html.
(151) Tarascon, J. M.; Armand, M. *Nature (insight review article)* **2001**, *414*, 359.
(152) Pushparaj, V. L.; Shaijumon, M. M.; Kumar, A.; Murugesan, S.; Ci, L.; Vajtai, R.; Linhardt, R. J.; Nalamasu, O.; Ajayan, P. M. *Proc. Natl. Acad. Sci. U.S.A.* **2007**, *104*, 13574.
(153) Srinivasan, V. http://berc.lbl.gov/venkat/(status of batteries for vehicles), 2008.
(154) Broussely, M.; Biensan, P.; Simon, B. *Electrochim. Acta* **1999**, *45*, 3.
(155) PNGV Battery Test Manual, Revision 3, DOE/ID105972001, February.
(156) Smith, K.; Wang, C.-Y. *J. Power Sources* **2006**, *160*, 662.
(157) Sudant, G.; Baudrin, E.; Larcher, D.; Tarascon, J.-M. *J. Mater. Chem.* **2005**, *15*, 1263.
(158) Armstrong, G.; Armstrong, A. R.; Canalas, J.; Bruce, P. G. *Electrochem. Solid-State Lett.* **2006**, *9*, A139.
(159) Polzot, P.; Laruelle, S.; Grugeon, S.; Dupont, L.; Tarascon, J.-M. *Nature (London)* **2000**, *407*, 496.
(160) Taberna, P. L.; Mitra, S.; Poizot, P.; Simon, P.; Tarascon, J.-M. *Nat. Mater.* **2006**, *5*, 568.
(161) Chen, W. X.; Lee, J. Y.; Liu, Z. L. *Carbon* **2003**, *41*, 959.
(162) Ishihara, T.; Nakasu, M.; Yoshio, M.; Nishiguchi, H.; Takita, Y. *J. Power Sources* **2005**, *146*, 161.
(163) Liu, P.; Lee, S. H.; Yan, Y. F.; Gennett, T.; Landi, B. J.; Dillon, A. C.; Heben, M. J. *Electrochem. Solid State Lett.* **2004**, *7*, A421.
(164) Pushparaj, V. L.; Shaijumon, M. M.; Kumar, A.; Murugesan, S.; Ci, L.; Vajtai, R.; Linhardt, R. J.; Nalamasu, O.; Ajayan, P. M. *Proc. Natl. Acad. Sci. U.S.A.* **2007**, *104*, 13574.
(165) Kawasaki, S.; Iwai, Y.; Hirose, M. *Carbon* **2009**, *47*, 1081.
(166) Smith, B. W.; Monthioux, M.; Luzzi, D. E. *Nature* **1998**, *396*, 323.
(167) Reddy, A. L. M.; Shaijumon, M. M.; Gowda, S. R.; Ajayan, P. M. *Nano Lett.* **2009**, *9*, 1002.
(168) Ban, C.; Wu, Z.; Gillaspie, D. T.; Chen, L.; Yan, Y.; Blackburn, J. L.; Dillon, A. C. *Adv. Mater.*, in press.
(169) Frackowiak, E.; Metenier, K.; Bertagna, V.; Beguin, F. *Appl. Phys. Lett.* **2000**, *77*, 2421.
(170) An, K. H.; Kim, W. S.; Park, Y. S.; Choi, Y. C.; Lee, S. M.; Chung, D. C.; Bae, D. J.; Lim, S. C.; Lee, Y. H. *Adv. Mater.* **2001**, *13*, 497.

(171) Kozlov, M. E.; Capps, R. C.; Sampson, W. M.; Ebron, V. H.; Ferraris, J. P.; Baughman, R. H. *Adv. Mater.* **2005**, *17*, 614.
(172) Du, C. S.; Pan, N. *J. Power Sources* **2006**, *160*, 1487–1494.
(173) Taberna, P. L.; Chevallier, G.; Simon, P.; Plee, D.; Aubert, T. *Mater. Res. Bull.* **2006**, *41*, 478.
(174) Futaba, D. N.; Hata, K.; Yamada, T.; Hiraoka, T.; Hayamizu, Y.; Kakudate, Y.; Tanaike, O.; Hatori, H.; Yumura, M.; Iijima, S. *Nat. Mater.* **2006**, *5*, 987.
(175) Hata, K.; Futaba, D. N.; Mizuno, K.; Namai, T.; Yumura, M.; Iijima, S. *Science* **2004**, *306*, 1362.
(176) Futaba, D. N.; Hata, K.; Namai, T.; Yamada, T.; Mizuno, K.; Hayamizu, Y.; Yumura, M.; Iijima, S. *J. Phys. Chem. B* **2006**, *110*, 8035.
(177) Pan, H.; Poh, C. K.; Feng, Y. P.; Lin, J. Y. *Chem. Mater.* **2007**, *19*, 6120.
(178) Huang, C. W.; Chuang, C. M.; Ting, J. M.; Teng, H. S. *J. Power Sources* **2008**, *183*, 406.
(179) Huang, C. W.; Teng, H. S. *J. Electrochem. Soc.* **2008**, *155*−A739.
(180) Nichols, W. T.; Keto, J. W.; Henneke, D. E.; Brock, J. R.; Malyavanatham, G.; Becker, M. F.; Glicksman, H. D. *Appl. Phys. Lett.* **2001**, *78*, 1128.
(181) Hashimoto, A.; Suenaga, K.; Gloter, A.; Urita, K.; Iijima, S. *Nature* **2004**, *430*, 870.

CR9003314